Fully Distributed Joint Localization and Target Tracking With Mobile Robot Networks

Pengxiang Zhu and Wei Ren, *Fellow, IEEE*

Abstract—In this article, we study the problem of joint localization and target tracking using a mobile robot network. Here, a team of mobile robots equipped with onboard sensors simultaneously localize themselves and track multiple targets. We introduce a fully distributed algorithm that is applicable to generic robot motion, target process, and measurement models and is robust to time-varying sensing and communication topologies and changing blind robots (the robots not directly sensing the targets). Instead of treating localization and target tracking as two separate problems, we explicitly account for the influence of one to the other and exploit it to improve performance in a fully distributed context. Two novel kinds of distributed estimates are derived. By employing them, each robot can estimate the pose (position and orientation) of itself (localization) and the states of targets (tracking) using only its local information and information from its one-hop communicating neighbors while preserving consistency. Furthermore, it is proven that, in the case of linear time-varying models, the estimation errors are bounded in the mean-square sense under very mild conditions on the sensing and communication graph and system observability. The effectiveness of our approach is demonstrated extensively through Monte Carlo simulations, and experiments carried out using a real-world data set. It is also shown better performance in the pose estimates of the robots is achieved when jointly estimating the robots' poses and targets' states.

Index Terms—Cooperative localization (CL), distributed estimation, Kalman filter, multi-robot systems, target tracking.

I. INTRODUCTION

SENSOR networks with the ability to communicate, sense, and interact with surroundings have a wide range of applications, such as region monitoring, area surveillance, and search and rescue. When mobile robots equipped with sensors are employed, a large area can be covered without the need to increase the number of sensors in the network. In addition, the robots can actively pursue targets and prevent them from escaping the sensing regions of their onboard sensors. In this article, a team of, possibly heterogeneous, mobile robots is employed to track multiple targets in a fully or intermittently absolute measurement (e.g., GPS data) denied environment. To perform this task,

distributed strategies outperform centralized approaches in scalability, energy (e.g., processing and communication) efficiency, and robustness against failures or attacks. In particular, we aim to propose a fully distributed algorithm with only local information and local communication in the absence of global parameters and multihop information propagation or flooding. As we do not assume *a priori* known information about the robots' poses, to successfully track the targets, it is necessary for the robots to determine their poses precisely. Cooperative localization (CL) is a widely used technique to achieve multirobot localization in the absence of absolute measurements. In CL, by cooperating with other robots, each robot can estimate its own pose using relative measurements (e.g., relative distance, bearing, relative pose, or any combination of them) between robots. In particular, distributed CL has gathered significant attention in robotics. However, distributed centralized-equivalent algorithms presented in [1]–[5] are not fully distributed. At each occurrence of the measurements, some variables need to be shared among the team through information propagation rather than purely one-hop neighbor-to-neighbor communication. For example, a distributed algorithm equivalent to the centralized *extended Kalman filter* (EKF) is presented in [1]. But the measurements obtained by one robot are required to be transmitted to all teammates. For another instance, [2] introduces new intermediate local variables to decouple the propagation stage of the EKF. However, the communication graph is required to have a spanning tree rooted at the interim master in order to propagate the intermediate local variables to the rest of the team through multiple hops in one time step. To relax the communication limitations in centralized-equivalent approaches, [6] presents an EKF-based distributed algorithm to handle asynchronous communication. But the cross correlations between robots are ignored, which leads to inconsistent estimates. In contrast, the distributed algorithm proposed in [7] is able to approximate the cross correlations between robots. Nevertheless, the estimate is not guaranteed to be consistent. The *covariance intersection* (CI) technique is used in [8] to compute a consistent estimate. However, the estimate requires a particular measurement model, specifically, the relative poses of neighbors. The *interleaved update* (IU) algorithm in [9] can handle generic models and compute consistent estimates. Nevertheless, each robot in a team of M robots has to maintain 2^M filters and keep tracking the origin of the measurements. Besides the above-mentioned limitations, all the aforementioned approaches do not consider robots working in a dynamic environment where moving targets exist and hence ignore the effect resulting

from jointly estimating the targets' states. In addition, there exist some cases where robots need to co-work with targets (e.g., humans), and then it is essential to estimate the poses of targets in addition to localizing themselves.

In another aspect, many algorithms have been proposed to address the distributed target estimation problem with sensor networks. Each sensor fuses local information with information from its neighbors to estimate the state of a common target. Current approaches, either consensus-based or diffusion-based algorithms, solve the tracking problem using a static sensor network, where the sensors' positions are assumed to be known explicitly or implicitly [10]–[18].

However, there exist several approaches to solving the problem of joint localization and target tracking (JLATT). Mobile robots are adopted in [19]–[21]. A consistent *unscented incremental smoothing* algorithm is introduced in [19] by enforcing the observability constraint on the unscented transformation. In [20], the problem is modeled under a least square minimization framework, where the states of the robots, the targets, and static landmarks are jointly estimated. To mitigate, not avoid, the risk of using the measurements more than once, a common reference is defined by using static landmarks which might be unavailable. By assuming that robots have access to the measurements of absolute orientations, an EKF-based approach is presented in [21]. Furthermore, it is analytically shown that jointly estimating the robot and target positions results in better accuracy of the robots' position estimates in the steady state, in comparison with the CL. It is worth noting that the algorithms mentioned earlier are all *centralized*.

A distributed algorithm for JLATT is presented in [22], where static sensors are used. The sensors are localized via a Jacobi algorithm that computes the *best linear unbiased estimates* in a distributed matter. In order to use the Jacobi algorithm, the measurements between sensors are required to have a particular linear model. In addition, each sensor has to maintain a history of the average measurements. As the number of sensors increases, the storage and computational costs increase dramatically. In addition, a distributed Kalman filter is designed to estimate the target's state. Here, only the prior estimates from neighbors are used, and the neighbors' relative measurements to the target are neglected. As a result, some useful information might be lost. Although this approach is distributed, it is limited to static sensor networks where each sensor's state is a static parameter to be estimated. When a mobile robot network is employed, each robot propagates its pose according to a noisy motion model. The state estimates of two robots or one robot and one target become correlated after updating the estimates using the relative measurements between them. Note that directly fusing these two estimates would yield an inconsistent estimate. Then, there exist significant challenges to avoid information double-counting between robots and account for the coupling between localization and target tracking.

The earlier observations motivate us to derive a fully distributed algorithm for JLATT with mobile robot networks. We explicitly account for the mutual influence between localization and target tracking and exploit it to improve performance in a fully distributed way. In terms of stability analysis,

it is worth pointing out that a few works analyze the stability in CL, while all the works on target tracking are limited to static sensor networks. We aim to jointly analyze the stability in both the localization and tracking parts. Our approach is based on two fully distributed estimates and able to track multiple targets by using mobile robots whose poses are unknown. The main contributions are summarized as follows.

1) To the best of our knowledge, it is the first time that a distributed algorithm with a consistency guarantee is proposed for JLATT in mobile robot networks. Each robot only needs to exchange information with its one-hop communicating neighbors.

2) The algorithm can handle multiple measurements simultaneously, including multiple relative measurements (i.e., robot-to-robot and robot-to-target measurements) and absolute measurements if available. Furthermore, it supports generic robot motion, target process, and measurement models.

3) In the case of linearized time-varying systems, it is proven that the estimated error covariances of both robots' poses and targets' states are bounded under certain mild conditions on the sensing and communication graphs and system observability. To the best of our knowledge, it is the first time that the stability for CL or JLATT in mobile robot networks is analyzed in a distributed setting, even for the linearized system.

Some preliminary results of this article are presented in our previous conference article [23]. Compared with this prior article, first, we introduce an alternative update strategy to guarantee consistency instead of using IU, which requires more storage and higher communication and computational costs. Second, robot-to-target measurements are fused with the prior estimates of robot poses. As a result, better accuracy in the robot pose estimates is achieved. In addition, we theoretically demonstrate the consistency and stability of the proposed algorithm under certain conditions and further present experimental evaluations with a real-world data set.

II. PRELIMINARIES

A. Notations and Definitions

Let the vector $\mathbf{x}^k$ represent the actual pose of a robot or the actual state of a target at time k. Given a real-valued $\mathbf{x}^k$, the prior estimate is $\bar{\mathbf{x}}^k$ and the posterior estimate is $\hat{\mathbf{x}}^k$. Denote, respectively, $\bar{\mathbf{e}}^k = \mathbf{x}^k - \bar{\mathbf{x}}^k$ and $\mathbf{e}^k = \mathbf{x}^k - \hat{\mathbf{x}}^k$, the prior and posterior estimation errors. Then, we use $\bar{\mathbf{p}}^k$ and $\mathbf{p}^k$ to represent, respectively, the estimated covariance of $\bar{\mathbf{e}}^k$ and $\mathbf{e}^k$. We distinguish the variables associated with robot i's self-estimate by the subscript R_i, e.g., $\bar{\mathbf{x}}^k_{R_i}$ representing robot i's prior estimate of its own actual pose $\mathbf{x}^k_{R_i}$ and $\bar{\mathbf{p}}^k_{R_i}$ representing the estimated covariance of $\bar{\mathbf{e}}^k_{R_i}$ with $\bar{\mathbf{e}}^k_{R_i} = \mathbf{x}^k_{R_i} - \bar{\mathbf{x}}^k_{R_i}$. Furthermore, we distinguish the variables associated with robot i's estimate of target j by the subscript T_{ij}, e.g., $\bar{\mathbf{x}}^k_{T_{ij}}$ denoting robot i's prior estimate of target j's actual state $\mathbf{x}^k_{T_j}$ and $\bar{\mathbf{p}}^k_{T_{ij}}$ denoting the estimated covariance of $\bar{\mathbf{e}}^k_{T_{ij}}$ with $\bar{\mathbf{e}}^k_{T_{ij}} = \mathbf{x}^k_{T_j} - \bar{\mathbf{x}}^k_{T_{ij}}$.

We denote by $\mathbf{I}_n$ the identity matrix of dimension $n \times n$. The superscript $\top$ denotes transpose and superscript -1 represents inverse. $\mathbb{E}\{\cdot\}$ computes the expectation of a random variable.

Diag$\{\cdot\}$ and Max$\{\cdot\}$ denote, respectively, the block-diagonal matrix constructed from the elements and the maximum of the elements. We let Tr$\{\cdot\}$ denote the trace of a matrix. The interval of time instants $\mathcal{T}_{k_0}^{k_n}$ is defined as $[k_0, \ldots, k_n]$, where $0 \leq k_0 < k_n < \infty$. For symmetric matrices $\mathbf{A}$ and $\mathbf{B}$, the notation $\mathbf{A} \geq \mathbf{B}$ (or $\mathbf{A} > \mathbf{B}$) means that $\mathbf{A} - \mathbf{B}$ is positive semidefinite (or definite). For finite sets $\mathcal{A}$ and $\mathcal{B}$, we denote by $\mathcal{A}\backslash\mathcal{B}$ the set whose elements include all elements in $\mathcal{A}$ that are not in $\mathcal{B}$. The transition matrix on $\mathcal{T}_{k_0}^{\tau}$, $\Phi(\tau, k_0)$, is defined as $\Phi(\tau, k_0) = \Phi_{R_i}^{\tau-1}, \ldots, \Phi_{R_i}^{k_0+1}\Phi_{R_i}^{k_0}$ and $\Phi(k_0, k_0)$ is the identity matrix.

Definition 1 [24]: Suppose that $\mathbf{x}^k$ is a random variable. Let $\hat{\mathbf{x}}^k$ and $\mathbf{p}^k$ be, respectively, the estimate of $\mathbf{x}^k$ and the estimated error covariance. The pair $(\hat{\mathbf{x}}^k, \mathbf{p}^k)$ is said to be consistent if the actual error covariance $\mathbb{E}\{\mathbf{e}^k(\mathbf{e}^k)^{\mathsf{T}}\} \leq \mathbf{p}^k$.

The consistency is a critical property of estimates that the estimated error covariances realistically express the covariance of actual errors. In contrast, an inconsistent estimate that underestimates the actual errors might diverge as a result [25], [26].

B. Graphs

In the network of M robots, we define a directed communication graph $G_c^k = (\mathcal{V}, \mathcal{E}_c^k)$, where $\mathcal{V} = \{R_1, \ldots, R_M\}$ is the robot set and $\mathcal{E}_c^k \subseteq \mathcal{V} \times \mathcal{V}$ is the edge set, which stands for the communication links between robots at time k. We assume that self-edge $(i, i) \in \mathcal{E}_c^k, \forall i \in \mathcal{V}$, exists in the communication graph. If there exists an edge $(j, i) \in \mathcal{E}_c^k$, where $j \neq i$, which means that robot i can receive information from robot j, then robot j is a communicating neighbor of robot i. At time k, the communicating neighbor set of robot i is defined as $\mathcal{N}_{c,i}^k = \{i|(l, i) \in \mathcal{E}_c^k, \forall l \neq i, l \in \mathcal{V}\}$; The inclusive communicating neighbor set of robot i is $\mathcal{J}_{c,i}^k = \mathcal{N}_{c,i}^k \cup \{i\}$.

Similarly, we define a directed sensing graph $G_s^k = (\mathcal{V}, \mathcal{E}_s^k)$ to describe robot-to-robot measurements, where $\mathcal{E}_s^k \subseteq \mathcal{V} \times \mathcal{V}$ is the edge set, which stands for the detection links between robots at time k. For example, when robot i detects robot j at time k, there exists an edge (j, i) directed from robot j to robot i in $\mathcal{E}_s^k$. At time k, we denote the sensing neighbor set of robot i by $\mathcal{N}_{s,i}^k = \{i|(l, i) \in \mathcal{E}_s^k, \forall l \neq i, l \in \mathcal{V}\}$ (i.e., all robots detected by robot i). A directed path is a sequence of edges in a directed graph of the form $(i_0, i_1), (i_1, i_2), \ldots$, where $i_j \in \mathcal{V}$. Besides, the set of N targets is denoted by $\mathcal{U} = \{T_1, \ldots, T_N\}$ and the subset of targets detected by robot i at time k is denoted by $\mathcal{U}_i^k$. We assume that for each robot, the communication radius is larger than the sensing radii of all robots. Then, when robot i detects robot j, robot i can receive the information broadcast by robot j.

C. Track-to-Track Fusion

Track-to-track fusion is the problem of combining multiple estimates of a state into a single and more accurate estimate. At time k, consider two consistent estimation pairs $(\mathbf{p}_{a_1}^k, \hat{\mathbf{x}}_{a_1}^k)$ and $(\mathbf{p}_{a_2}^k, \hat{\mathbf{x}}_{a_2}^k)$ of $\mathbf{x}^k$, we seek to compute an improved consistent estimate $(\mathbf{p}_c^k, \hat{\mathbf{x}}_c^k)$. The cross correlation between $\hat{\mathbf{x}}_{a_1}^k$ and $\hat{\mathbf{x}}_{a_2}^k$ is denoted as $\mathbf{p}_{a_1 a_2}^k$. If $\mathbf{p}_{a_1 a_2}^k$ is known, the consistent fused

estimate with minimum covariance is given by [27]

$$\mathbf{p}_c^k = \mathbf{p}_{a_1}^k - (\mathbf{p}_{a_1}^k - \mathbf{p}_{a_1 a_2}^k)$$
$$\times [\mathbf{p}_{a_1}^k + \mathbf{p}_{a_2}^k - \mathbf{p}_{a_1 a_2}^k - (\mathbf{p}_{a_1 a_2}^k)^{\mathsf{T}}]^{-1}[\mathbf{p}_{a_1}^k - (\mathbf{p}_{a_1 a_2}^k)^{\mathsf{T}}]$$
$$\hat{\mathbf{x}}_c^k = \hat{\mathbf{x}}_{a_1}^k + (\mathbf{p}_{a_1}^k - \mathbf{p}_{a_1 a_2}^k)$$
$$\times [\mathbf{p}_{a_1}^k + \mathbf{p}_{a_2}^k - \mathbf{p}_{a_1 a_2}^k - (\mathbf{p}_{a_1 a_2}^k)^{\mathsf{T}}]^{-1}(\hat{\mathbf{x}}_{a_2}^k - \hat{\mathbf{x}}_{a_1}^k).$$

Furthermore, if $\hat{\mathbf{x}}_{a_1}^k$ and $\hat{\mathbf{x}}_{a_2}^k$ are independent, by setting $\mathbf{p}_{a_1 a_2}^k = 0$, we have

$$(\mathbf{p}_c^k)^{-1} = (\mathbf{p}_{a_1}^k)^{-1} + (\mathbf{p}_{a_2}^k)^{-1}$$
$$\hat{\mathbf{x}}_c^k = \mathbf{p}_c^k[(\mathbf{p}_{a_1}^k)^{-1}\hat{\mathbf{x}}_{a_1}^k + (\mathbf{p}_{a_2}^k)^{-1}\hat{\mathbf{x}}_{a_2}^k]. \tag{1}$$

On the other hand, if $\mathbf{p}_{a_1 a_2}^k$ is unknown, CI, a well-known conservative fusion scheme that yields a consistent fused estimate, is given as follows [24]:

$$[\mathbf{p}_c^k]_{\text{CI}} = [\alpha_1^k(\mathbf{p}_{a_1}^k)^{-1} + (1 - \alpha_1^k)(\mathbf{p}_{a_2}^k)^{-1}]^{-1}$$
$$[\hat{\mathbf{x}}_c^k]_{\text{CI}} = [\mathbf{p}_c^k]_{\text{CI}}[\alpha_1^k(\mathbf{p}_{a_1}^k)^{-1}\hat{\mathbf{x}}_{a_1}^k + (1 - \alpha_1^k)(\mathbf{p}_{a_2}^k)^{-1}\hat{\mathbf{x}}_{a_2}^k] \tag{2}$$

where $\alpha_1^k \in [0, 1]$. Compared with CI, the recently proposed *inverse CI* (ICI) [28] provides an optimal consistent and tight solution, and therefore, is more accurate. The ICI is given as [28]

$$[\mathbf{p}_c^k]_{\text{ICI}} = [(\mathbf{p}_{a_1}^k)^{-1} + (\mathbf{p}_{a_2}^k)^{-1} - (\Gamma_c^k)^{-1}]^{-1}$$
$$[\hat{\mathbf{x}}_c^k]_{\text{ICI}} = [\mathbf{p}_c^k]_{\text{ICI}}(\mathbf{K}_c^k\hat{\mathbf{x}}_{a_1}^k + \mathbf{L}_c^k\hat{\mathbf{x}}_{a_2}^k) \tag{3}$$

where

$$\Gamma_c^k = \alpha_2^k\mathbf{p}_{a_1}^k + (1 - \alpha_2^k)\mathbf{p}_{a_2}^k$$
$$\mathbf{K}_c^k = (\mathbf{p}_{a_1}^k)^{-1} - \alpha_2^k(\Gamma_c^k)^{-1}$$
$$\mathbf{L}_c^k = (\mathbf{p}_{a_2}^k)^{-1} - (1 - \alpha_2^k)(\Gamma_c^k)^{-1}$$

for any $\alpha_2^k \in [0, 1]$. The time-varying parameters α_1^k and α_2^k can be chosen to minimize an optimality criterion, such as the traces of $[\mathbf{p}_c^k]_{\text{CI}}$ and $[\mathbf{p}_c^k]_{\text{ICI}}$, respectively. $(\Gamma_c^k)^{-1}$ can be considered a tight outer bound of the common information.

Lemma 1 [28]: Let $[\mathbf{p}_c^k]_{\text{CI}}^*$ and $[\mathbf{p}_c^k]_{\text{ICI}}^*$ be, respectively, the fused covariances with minimal traces by using CI and ICI at time k. Then, $[\mathbf{p}_c^k]_{\text{ICI}}^* \leq [\mathbf{p}_c^k]_{\text{CI}}^*$.

CI is generalized to fuse an arbitrary number of estimation pairs $(\mathbf{p}_{a_i}^k, \hat{\mathbf{x}}_{a_i}^k)$, $i = 1, \ldots, n$, according to [29]

$$[\mathbf{p}_c^k]_{\text{CI}} = \left[\sum_{i=1}^n \alpha_i^k(\mathbf{p}_{a_i}^k)^{-1}\right]^{-1}$$
$$[\hat{\mathbf{x}}_c^k]_{\text{CI}} = [\mathbf{p}_c^k]_{\text{CI}}\left[\sum_{i=1}^n \alpha_i^k(\mathbf{p}_{a_i}^k)^{-1}\hat{\mathbf{x}}_{a_i}^k\right] \tag{4}$$

where $\alpha_i^k \in [0, 1]$ and $\sum_{i=1}^n \alpha_i^k = 1$. For the sake of computational simplicity, we use the simplified algorithm in [30] to calculate α_i^k as

$$\alpha_i^k = \frac{1/\text{Tr}\{\mathbf{p}_{a_i}^k\}}{\sum_{i=1}^n 1/\text{Tr}\{\mathbf{p}_{a_i}^k\}}. \tag{5}$$

D. Problem Formulation

Consider a group of M heterogeneous mobile robots and N targets moving within the same space. Each robot carries proprioceptive sensors (e.g., odometries) to measure its self-motion and exteroceptive sensors (e.g., cameras or laser scanners) to generate relative measurements to other robots and multiple targets. Besides, some robots might have access to the absolute measurements intermittently. The motion of robot i is described by a nonlinear model

$$\mathbf{x}_{R_i}^k = \mathbf{f}_i\left(\mathbf{x}_{R_i}^{k-1}, \mathbf{u}_{R_i}^{k-1} - \mathbf{w}_{R_i}^{k-1}\right) \tag{6}$$

where $\mathbf{x}_{R_i}^k$, $\mathbf{u}_{R_i}^k$, and $\mathbf{w}_{R_i}^k$ are, respectively, the ith robot's pose (position and orientation), the measured input, and the process noise at time k. We assume that the noise $\mathbf{w}_{R_i}$ is zero-mean white Gaussian.

The state of target j at time k is represented by $\mathbf{x}_{T_j}^k$, which might contain the target's pose or velocity components. The process model of target j is given as

$$\mathbf{x}_{T_j}^k = \mathbf{g}_j\left(\mathbf{x}_{T_j}^{k-1}, \mathbf{w}_{T_j}^{k-1}\right) \tag{7}$$

where $\mathbf{w}_{T_j}$ is the process noise, assumed to be zero-mean white Gaussian.

At time k, if robot j (respectively, target j) is within the sensing region of robot i, robot i obtains the robot-to-robot measurement $\mathbf{z}_{R_{ij}}^k$ (respectively, robot-to-target measurement $\mathbf{z}_{T_{ij}}^k$). If accessible, robot i receives the absolute measurement $\mathbf{z}_{R_i}^k$. We model the collected measurements as

$$\begin{aligned}\mathbf{z}_{R_{ij}}^k &= \mathbf{h}_{ij}^r\left(\mathbf{x}_{R_i}^k, \mathbf{x}_{R_j}^k\right) + \mathbf{v}_{R_{ij}}^k \\ \mathbf{z}_{T_{ij}}^k &= \mathbf{h}_{ij}^t\left(\mathbf{x}_{R_i}^k, \mathbf{x}_{T_j}^k\right) + \mathbf{v}_{T_{ij}}^k \\ \mathbf{z}_{R_i}^k &= \mathbf{h}_i^a\left(\mathbf{x}_{R_i}^k\right) + \mathbf{v}_{R_i}^k\end{aligned} \tag{8}$$

where $\mathbf{v}_{R_{ij}}^k$, $\mathbf{v}_{T_{ij}}^k$, and $\mathbf{v}_{R_i}^k$ are the corresponding measurement noises, assumed to be zero-mean white Gaussian. The covariance matrices are, respectively, represented as $\mathbf{R}_{R_{ij}}^k = \mathbf{E}[\mathbf{v}_{R_{ij}}^k(\mathbf{v}_{R_{ij}}^k)^{\mathsf{T}}]$, $\mathbf{R}_{T_{ij}}^k = \mathbf{E}[\mathbf{v}_{T_{ij}}^k(\mathbf{v}_{T_{ij}}^k)^{\mathsf{T}}]$, and $\mathbf{R}_{R_i}^k = \mathbf{E}[\mathbf{v}_{R_i}^k(\mathbf{v}_{R_i}^k)^{\mathsf{T}}]$. Note that at any time, some robots might not be able to obtain any relative or absolute measurement. Furthermore, we assume that the measurement noises are mutually uncorrelated across robots and are uncorrelated with the process noises.

The objective of our work is for each robot i to construct estimates of its own pose and of each target's state by using its local measurements if available and the information received from its one-hop communicating neighbors at the current time.

III. PROPOSED FULLY DISTRIBUTED ALGORITHM

In this section, we derive a fully distributed scheme for JLATT from the perspective of *extended information filter* (EIF), the information form of the Kalman filter.

A. Distributed Extended Information Filtering

1) Localization: Unlike the existing works on distributed target estimation with static sensor networks where the pose of each sensor is deterministic and known, we consider the general scenario where the poses of the mobile robots (serving as mobile sensors) are states to be estimated.

Robot i estimates $\mathbf{x}_{R_i}^k$ by using its available relative measurements to other robots and targets. At time k, when robot i detects another robot $l \in \mathcal{V}$, robot i obtains the relative measurement $\mathbf{z}_{R_{il}}^k$ and receives the information broadcast by robot l. The broadcast information contains robot l's current pose estimate $\bar{\mathbf{x}}_{R_l}^k$ with estimated covariance $\bar{\mathbf{p}}_{R_l}^k$. After linearization of the measurement $\mathbf{z}_{R_{il}}^k$ at $\bar{\mathbf{x}}_{R_i}^k$ and $\bar{\mathbf{x}}_{R_l}^k$, we compute the measurement residual

$$\bar{\mathbf{z}}_{R_{il}}^k = \mathbf{H}_{R_{il}}^k \bar{\mathbf{e}}_{R_i}^k + \widetilde{\mathbf{H}}_{R_{il}}^k \bar{\mathbf{e}}_{R_l}^k + \mathbf{v}_{R_{il}}^k \tag{9}$$

where $\bar{\mathbf{z}}_{R_{il}}^k = \mathbf{z}_{R_{il}}^k - \mathbf{h}_{il}^r(\bar{\mathbf{x}}_{R_i}^k, \bar{\mathbf{x}}_{R_l}^k)$ with $\mathbf{H}_{R_{il}}^k = (\partial \mathbf{h}_{il}^r/\partial \mathbf{x}_{R_i})(\bar{\mathbf{x}}_{R_i}^k, \bar{\mathbf{x}}_{R_l}^k)$ and $\widetilde{\mathbf{H}}_{R_{il}}^k = (\partial \mathbf{h}_{il}^r/\partial \mathbf{x}_{R_l})(\bar{\mathbf{x}}_{R_i}^k, \bar{\mathbf{x}}_{R_l}^k)$. By defining $\bar{\mathbf{v}}_{R_{il}}^k = \widetilde{\mathbf{H}}_{R_{il}}^k \bar{\mathbf{e}}_{R_l}^k + \mathbf{v}_{R_{il}}^k$, we get

$$\bar{\mathbf{z}}_{R_{il}}^k = \mathbf{H}_{R_{il}}^k \bar{\mathbf{e}}_{R_i}^k + \bar{\mathbf{v}}_{R_{il}}^k.$$

The corresponding covariance for $\bar{\mathbf{v}}_{R_{il}}^k$ is given by

$$\bar{\mathbf{R}}_{R_{il}}^k = \mathbf{R}_{R_{il}}^k + \widetilde{\mathbf{H}}_{R_{il}}^k \bar{\mathbf{p}}_{R_l}^k \left(\widetilde{\mathbf{H}}_{R_{il}}^k\right)^{\mathsf{T}} \tag{10}$$

which has included the uncertainty of robot l's pose estimate. Then, define the relative correction pair $(\mathbf{s}_{R_{il}}^k, \mathbf{y}_{R_{il}}^k)$ as

$$\begin{aligned}\mathbf{s}_{R_{il}}^k &= \left(\mathbf{H}_{R_{il}}^k\right)^{\mathsf{T}}\left(\bar{\mathbf{R}}_{R_{il}}^k\right)^{-1}\mathbf{H}_{R_{il}}^k \\ \mathbf{y}_{R_{il}}^k &= \left(\mathbf{H}_{R_{il}}^k\right)^{\mathsf{T}}\left(\bar{\mathbf{R}}_{R_{il}}^k\right)^{-1}\left(\bar{\mathbf{z}}_{R_{il}}^k + \mathbf{H}_{R_{il}}^k \bar{\mathbf{x}}_{R_i}^k\right).\end{aligned} \tag{11}$$

Similarly, when robot i detects target $j \in \mathcal{U}$, robot i obtains the relative measurement $\mathbf{z}_{T_{ij}}^k$. After linearization of the measurement $\mathbf{z}_{T_{ij}}^k$ at $\bar{\mathbf{x}}_{R_i}^k$ and $\bar{\mathbf{x}}_{T_{ij}}^k$, we compute the measurement residual

$$\bar{\mathbf{z}}_{T_{ij}}^k = \mathbf{H}_{T_{ij}}^k \bar{\mathbf{e}}_{R_i}^k + \widetilde{\mathbf{H}}_{T_{ij}}^k \bar{\mathbf{e}}_{T_{ij}}^k + \mathbf{v}_{T_{ij}}^k \tag{12}$$

where $\bar{\mathbf{z}}_{T_{ij}}^k = \mathbf{z}_{T_{ij}}^k - \mathbf{h}_{ij}^t(\bar{\mathbf{x}}_{R_i}^k, \bar{\mathbf{x}}_{T_{ij}}^k)$ with $\mathbf{H}_{T_{ij}}^k = (\partial \mathbf{h}_{ij}^t/\partial \mathbf{x}_{R_i})(\bar{\mathbf{x}}_{R_i}^k, \bar{\mathbf{x}}_{T_{ij}}^k)$ and $\widetilde{\mathbf{H}}_{T_{ij}}^k = (\partial \mathbf{h}_{ij}^t/\partial \mathbf{x}_{T_{ij}})(\bar{\mathbf{x}}_{R_i}^k, \bar{\mathbf{x}}_{T_{ij}}^k)$. By defining $\bar{\mathbf{v}}_{T_{ij}}^k = \widetilde{\mathbf{H}}_{T_{ij}}^k \bar{\mathbf{e}}_{T_{ij}}^k + \mathbf{v}_{T_{ij}}^k$, we get

$$\bar{\mathbf{z}}_{T_{ij}}^k = \mathbf{H}_{T_{ij}}^k \bar{\mathbf{e}}_{R_i}^k + \bar{\mathbf{v}}_{T_{ij}}^k.$$

The corresponding covariance of $\bar{\mathbf{v}}_{T_{ij}}^k$ is given by

$$\bar{\mathbf{R}}_{T_{ij}}^k = \mathbf{R}_{T_{ij}}^k + \widetilde{\mathbf{H}}_{T_{ij}}^k \bar{\mathbf{p}}_{T_{ij}}^k \left(\widetilde{\mathbf{H}}_{T_{ij}}^k\right)^{\mathsf{T}}. \tag{13}$$

Then, define the relative correction pair $(\mathbf{s}_{T_{ij}}^k, \mathbf{y}_{T_{ij}}^k)$ as

$$\begin{aligned}\mathbf{s}_{T_{ij}}^k &= \left(\mathbf{H}_{T_{ij}}^k\right)^{\mathsf{T}}\left(\bar{\mathbf{R}}_{T_{ij}}^k\right)^{-1}\mathbf{H}_{T_{ij}}^k \\ \mathbf{y}_{T_{ij}}^k &= \left(\mathbf{H}_{T_{ij}}^k\right)^{\mathsf{T}}\left(\bar{\mathbf{R}}_{T_{ij}}^k\right)^{-1}\left(\bar{\mathbf{z}}_{T_{ij}}^k + \mathbf{H}_{T_{ij}}^k \bar{\mathbf{x}}_{R_i}^k\right).\end{aligned} \tag{14}$$

Note that unlike (11), no communication is needed to compute (14) as $(\bar{\mathbf{p}}_{T_{ij}}^k, \bar{\mathbf{x}}_{T_{ij}}^k)$, $\bar{\mathbf{x}}_{R_i}^k$, and $\mathbf{z}_{T_{ij}}^k$ are all available at robot i.

Remark 1: As shown in (10) and (13), the noise covariances $\mathbf{R}_{R_{il}}^k$ and $\mathbf{R}_{T_{ij}}^k$ are, respectively, suitably increased by a positive semidefinite quantity $\widetilde{\mathbf{H}}_{R_{il}}^k \bar{\mathbf{p}}_{R_l}^k (\widetilde{\mathbf{H}}_{R_{il}}^k)^{\mathsf{T}}$ and $\widetilde{\mathbf{H}}_{T_{ij}}^k \bar{\mathbf{p}}_{T_{ij}}^k (\widetilde{\mathbf{H}}_{T_{ij}}^k)^{\mathsf{T}}$. As a result, a large uncertainty in robot l's pose or target j's state leads to a large $\bar{\mathbf{R}}_{R_{il}}^k$ or $\bar{\mathbf{R}}_{T_{ij}}^k$, which makes $(\mathbf{s}_{R_{il}}^k, \mathbf{y}_{R_{il}}^k)$ or $(\mathbf{s}_{T_{ij}}^k, \mathbf{y}_{T_{ij}}^k)$ small. Then, the influence caused by the corresponding inaccurate measurements will be alleviated.

At time k, if robot i has access to its absolute measurement $\mathbf{z}_{R_i}^k$, the measurement residual after linearization at $\bar{\mathbf{x}}_{R_i}^k$ is given by

$$\bar{\mathbf{z}}_{R_i}^k = \mathbf{C}_{R_i}^k \bar{\mathbf{e}}_{R_i}^k + \mathbf{v}_{R_i}^k \tag{15}$$

where $\bar{\mathbf{z}}_{R_i}^k = \mathbf{z}_{R_i}^k - \mathbf{h}_i^a(\bar{\mathbf{x}}_{R_i}^k)$ with $\mathbf{C}_{R_i}^k = (\partial \mathbf{h}_i^a/\partial \mathbf{x}_{R_i})(\bar{\mathbf{x}}_{R_i}^k)$. For notation convenience, if robot i's absolute measurement is not accessible, we let $\mathbf{R}_{R_i}^k = \infty$, which assumes infinite uncertainty about $\mathbf{z}_{R_i}^k$. Then, we denote the absolute correction pair $(\mathbf{s}_{R_{ii}}^k, \mathbf{y}_{R_{ii}}^k)$ as

$$\mathbf{s}_{R_{ii}}^k = (\mathbf{C}_{R_i}^k)^\top (\mathbf{R}_{R_i}^k)^{-1} \mathbf{C}_{R_i}^k$$
$$\mathbf{y}_{R_{ii}}^k = (\mathbf{C}_{R_i}^k)^\top (\mathbf{R}_{R_i}^k)^{-1} (\bar{\mathbf{z}}_{R_i}^k + \mathbf{C}_{R_i}^k \bar{\mathbf{x}}_{R_i}^k). \quad (16)$$

Next, the task is to compute the posterior estimate $\hat{\mathbf{x}}_{R_i}^k$ with the estimated covariance $\mathbf{p}_{R_i}^k$ from the available correction pairs and the prior estimate $\bar{\mathbf{x}}_{R_i}^k$ with the estimated covariance $\bar{\mathbf{p}}_{R_i}^k$. Although the relative measurement noises are mutually uncorrelated, the defined $\bar{\mathbf{v}}_{R_{il}}^k$ and $\bar{\mathbf{v}}_{T_{ij}}^k$ are correlated for different l and j due to the correlations between the estimates of the robots' poses and the targets' states. Accordingly, the corresponding relative correction pairs are correlated. We apply the CI algorithm (4) on the relative correction pairs to guarantee consistency with the simplified weight selection strategy (5). The absolute correction pair can be directly incorporated, as it is uncorrelated with the relative correction pairs. Therefore, at time k, we can compute an estimate of $\mathbf{x}_{R_i}^k$ by using all available correction pairs. We have

$$\check{\mathbf{p}}_{R_i}^k = \left(\sum_{l \in \mathcal{N}_{s,i}^k} \eta_{il}^k \mathbf{s}_{R_{il}}^k + \sum_{j \in \mathcal{U}_i^k} \eta_{ij}^k \mathbf{s}_{T_{ij}}^k + \mathbf{s}_{R_{ii}}^k \right)^{-1} \quad (17a)$$

$$\check{\mathbf{x}}_{R_i}^k = \check{\mathbf{p}}_{R_i}^k \left(\sum_{l \in \mathcal{N}_{s,i}^k} \eta_{il}^k \mathbf{y}_{R_{il}}^k + \sum_{j \in \mathcal{U}_i^k} \eta_{ij}^k \mathbf{y}_{T_{ij}}^k + \mathbf{y}_{R_{ii}}^k \right) \quad (17b)$$

where $\eta_{il}^k \in (0,1]$ and $\eta_{ij}^k \in (0,1]$ subject to $\sum_{l \in \mathcal{N}_{s,i}^k} \eta_{il}^k + \sum_{j \in \mathcal{U}_i^k} \eta_{ij}^k = 1$.

Recall that another estimate of $\mathbf{x}_{R_i}^k$ is the prior estimate $\bar{\mathbf{x}}_{R_i}^k$. Here, one might be tempted to directly fuse them using (1) as

$$\mathbf{p}_{R_i}^k = \left[(\bar{\mathbf{p}}_{R_i}^k)^{-1} + (\check{\mathbf{p}}_{R_i}^k)^{-1} \right]^{-1}$$
$$\hat{\mathbf{x}}_{R_i}^k = \mathbf{p}_{R_i}^k \left[(\bar{\mathbf{p}}_{R_i}^k)^{-1} \bar{\mathbf{x}}_{R_i}^k + (\check{\mathbf{p}}_{R_i}^k)^{-1} \check{\mathbf{x}}_{R_i}^k \right] \quad (18)$$

which implicitly assumes that $\bar{\mathbf{x}}_{R_i}^k$ and $\check{\mathbf{x}}_{R_i}^k$ are uncorrelated. However, this is not the case. For example, when robot i uses robot l's pose estimate to update its own, their estimates become correlated. If we use (18) directly, when there exists a chain of updates back to robot l, robot l's pose estimate will be overconfident, since we incorporate the common information twice. In fact, the posterior estimation process becomes the problem of track-to-track fusion under unknown correlations. In order to guarantee the consistency while improving the accuracy, we adopt an ICI-based update approach to fuse $\bar{\mathbf{x}}_{R_i}^k$ and $\check{\mathbf{x}}_{R_i}^k$ in this step. The proposed *distributed EIF* (DEIF) algorithm for localization is summarized in Table I.

Remark 2: We incorporate robot-to-target measurements $\mathbf{z}_{T_{ij}}^k$ in the localization part. Intuitively, this can result in more accurate estimates of the robots' poses, since the targets can be treated as moving references to the robots. This is one of the advantages resulting from jointly estimating the states of both robots and targets. The algorithm in Table I is still

TABLE I
DEIF ALGORITHM FOR LOCALIZATION

Propagation:
$$\mathbf{\Phi}_{R_i}^{k-1} = \frac{\partial \mathbf{f}_i}{\partial \mathbf{x}_{R_i}}(\hat{\mathbf{x}}_{R_i}^{k-1}, \mathbf{u}_{R_i}^{k-1}),$$
$$\mathbf{G}_{R_i}^{k-1} = \frac{\partial \mathbf{f}_i}{\partial \mathbf{w}_{R_i}}(\hat{\mathbf{x}}_{R_i}^{k-1}, \mathbf{u}_{R_i}^{k-1}),$$
$$\mathbf{Q}_{R_i}^{k-1} = \mathbf{G}_{R_i}^{k-1} \mathbf{E}[\mathbf{w}_{R_i}^{k-1}(\mathbf{w}_{R_i}^{k-1})^\top](\mathbf{G}_{R_i}^{k-1})^\top,$$
$$\bar{\mathbf{p}}_{R_i}^k = \mathbf{\Phi}_{R_i}^{k-1} \mathbf{p}_{R_i}^{k-1}(\mathbf{\Phi}_{R_i}^{k-1})^\top + \mathbf{Q}_{R_i}^{k-1},$$
$$\bar{\mathbf{x}}_{R_i}^k = \mathbf{f}_i(\hat{\mathbf{x}}_{R_i}^{k-1}, \mathbf{u}_{R_i}^{k-1}).$$

Compute the update terms:

Obtain $(\check{\mathbf{p}}_{R_i}^k, \check{\mathbf{x}}_{R_i}^k)$ using (10)-(17).
$$\mathbf{\Omega}_{R_i}^k = (\bar{\mathbf{p}}_{R_i}^k)^{-1}, \quad \mathbf{q}_{R_i}^k = (\bar{\mathbf{p}}_{R_i}^k)^{-1} \bar{\mathbf{x}}_{R_i}^k,$$
$$\mathbf{\Gamma}_{R_i}^k = (\check{\mathbf{p}}_{R_i}^k)^{-1}[\alpha_i^k(\check{\mathbf{p}}_{R_i}^k)^{-1} + (1-\alpha_i^k)\mathbf{\Omega}_{R_i}^k]^{-1}\mathbf{\Omega}_{R_i}^k,$$
$$\mathbf{K}_{R_i}^k = \mathbf{\Omega}_{R_i}^k - \alpha_i^k \mathbf{\Gamma}_{R_i}^k,$$
$$\mathbf{L}_{R_i}^k = (\check{\mathbf{p}}_{R_i}^k)^{-1} - (1-\alpha_i^k)\mathbf{\Gamma}_{R_i}^k.$$

Update:
$$\mathbf{p}_{R_i}^k = [\mathbf{\Omega}_{R_i}^k + (\check{\mathbf{p}}_{R_i}^k)^{-1} - \mathbf{\Gamma}_{R_i}^k]^{-1}$$
$$\hat{\mathbf{x}}_{R_i}^k = \mathbf{p}_{R_i}^k[\mathbf{K}_{R_i}^k(\mathbf{\Omega}_{R_i}^k)^{-1}\mathbf{q}_{R_i}^k + \mathbf{L}_{R_i}^k \check{\mathbf{x}}_{R_i}^k].$$

The time-varying weight α_i^k subject to $\alpha_i^k \in [0,1]$ is selected to minimize $\mathrm{Tr}\{\mathbf{p}_{R_i}^k\}$.

applicable in the case of CL without targets involved by simply letting $\mathcal{U}_i^k = \varnothing$ in (17). In this case, we refer to the algorithm as CL-DEIF. Compared with the existing works on CL, our approach is a fully distributed solution that is consistent, amenable to general models, and computationally simple while accounting for the possible existence of targets.

2) Target Tracking: Recall that when robot i detects target $j \in \mathcal{U}$ at time k, linearization of $\mathbf{z}_{T_{ij}}^k$ at $\bar{\mathbf{x}}_{T_{ij}}^k$ and $\bar{\mathbf{x}}_{R_i}^k$ yields the measurement residual (12). By defining $\tilde{\mathbf{v}}_{T_{ij}}^k = \mathbf{H}_{T_{ij}}^k \bar{\mathbf{e}}_{R_i}^k + \mathbf{v}_{T_{ij}}^k$, we get $\bar{\mathbf{z}}_{T_{ij}}^k = \widetilde{\mathbf{H}}_{T_{ij}}^k \bar{\mathbf{e}}_{T_{ij}}^k + \tilde{\mathbf{v}}_{T_{ij}}^k$. The corresponding covariance of $\tilde{\mathbf{v}}_{T_{ij}}^k$ is given by

$$\widetilde{\mathbf{R}}_{T_{ij}}^k = \mathbf{R}_{T_{ij}}^k + \mathbf{H}_{T_{ij}}^k \bar{\mathbf{p}}_{R_i}^k(\mathbf{H}_{T_{ij}}^k)^\top. \quad (19)$$

Then, define the relative correction pair $(\tilde{\mathbf{s}}_{T_{ij}}^k, \tilde{\mathbf{y}}_{T_{ij}}^k)$ as

$$\tilde{\mathbf{s}}_{T_{ij}}^k = (\widetilde{\mathbf{H}}_{T_{ij}}^k)^\top (\widetilde{\mathbf{R}}_{T_{ij}}^k)^{-1} \widetilde{\mathbf{H}}_{T_{ij}}^k$$
$$\tilde{\mathbf{y}}_{T_{ij}}^k = (\widetilde{\mathbf{H}}_{T_{ij}}^k)^\top (\widetilde{\mathbf{R}}_{T_{ij}}^k)^{-1} (\bar{\mathbf{z}}_{T_{ij}}^k + \widetilde{\mathbf{H}}_{T_{ij}}^k \bar{\mathbf{x}}_{T_{ij}}^k). \quad (20)$$

Next, all available prior estimation pairs and correction pairs from the inclusive communicating neighborhood, i.e., $(\bar{\mathbf{p}}_{T_{lj}}^k, \bar{\mathbf{x}}_{T_{lj}}^k)$ and $(\tilde{\mathbf{s}}_{T_{lj}}^k, \tilde{\mathbf{y}}_{T_{lj}}^k)$, $\forall l \in \mathcal{J}_{c,i}^k$, are incorporated to compute the posterior estimate $\hat{\mathbf{x}}_{T_{ij}}^k$ with the estimated covariance $\mathbf{p}_{T_{ij}}^k$. It is possible that a certain robot, say robot l, cannot directly detect target j. Then, for notation convenience, we let $\mathbf{R}_{T_{lj}}^k = \infty$, which assumes infinite uncertainty about the corresponding measurement $\mathbf{z}_{T_{lj}}^k$. As a result, the received $\tilde{\mathbf{y}}_{T_{lj}}^k = 0$ and $\tilde{\mathbf{s}}_{T_{lj}}^k = 0$.

The first step is to use all available correction pairs to compute an estimate of $\mathbf{x}_{T_j}^k$. Similar to the localization part, due to the correlations between the robot pose estimates, the defined $\check{\mathbf{v}}_{T_{ij}}^k$ are correlated for different i. Accordingly, we apply the CI algorithm (4) on the relative correction pairs to guarantee consistency with the simplified weight selection strategy (5). Then, at time k, by using all available relative correction pairs, we have

$$\check{\mathbf{p}}_{T_{ij}}^k = \left(\sum_{l\in\mathcal{J}_{c,i}^k}\tilde{\eta}_{lj}^k\tilde{\mathbf{s}}_{T_{lj}}^k\right)^{-1}$$
$$\check{\mathbf{x}}_{T_{ij}}^k = \check{\mathbf{p}}_{T_{ij}}^k\left(\sum_{l\in\mathcal{J}_{c,i}^k}\tilde{\eta}_{lj}^k\tilde{\mathbf{y}}_{T_{lj}}^k\right) \quad (21)$$

where $\tilde{\eta}_{lj}^k = 0$ if robot l cannot directly detect target j; otherwise $\tilde{\eta}_{lj}^k \in (0,1]$ is the weight subject to $\sum_{l\in\mathcal{J}_{c,i}^k}\tilde{\eta}_{lj}^k = 1$. The second step is to fuse all available prior estimation pairs. Due to the common process model of target j, the local prior estimates $(\bar{\mathbf{p}}_{T_{lj}}^k, \bar{\mathbf{x}}_{T_{lj}}^k)$, $\forall l \in \mathcal{J}_{c,i}^k$, are highly correlated after propagations. Therefore, the CI algorithm (4) is used to guarantee consistency with the simplified weight selection strategy (5). We have

$$\Omega_{T_{ij}}^k = \sum_{l\in\mathcal{J}_{c,i}^k}\pi_{il}^k\left(\bar{\mathbf{p}}_{T_{lj}}^k\right)^{-1}$$
$$\mathbf{q}_{T_{ij}}^k = \sum_{l\in\mathcal{J}_{c,i}^k}\pi_{il}^k\left(\bar{\mathbf{p}}_{T_{lj}}^k\right)^{-1}\bar{\mathbf{x}}_{T_{lj}}^k \quad (22)$$

where $\pi_{il}^k \geq \underline{\pi} > 0$ is the weight subject to $\sum_{l\in\mathcal{J}_{c,i}^k}\pi_{il}^k = 1$ with $\underline{\pi}$ being the uniform lower bound of all the weights at all time steps.

The third step is to fuse $(\check{\mathbf{p}}_{T_{ij}}^k, \check{\mathbf{x}}_{T_{ij}}^k)$ with $(\Omega_{T_{ij}}^k, \mathbf{q}_{T_{ij}}^k)$ to compute the posterior estimate of target j. One might consider that the relative correction pairs and the prior estimation pairs are uncorrelated and directly fuse $(\check{\mathbf{p}}_{T_{ij}}^k, \check{\mathbf{x}}_{T_{ij}}^k)$ with $(\Omega_{T_{ij}}^k, \mathbf{q}_{T_{ij}}^k)$ using (1) as

$$\mathbf{p}_{T_{ij}}^k = \left[\Omega_{T_{ij}}^k + \left(\check{\mathbf{p}}_{T_{ij}}^k\right)^{-1}\right]^{-1}$$
$$\hat{\mathbf{x}}_{T_{ij}}^k = \mathbf{p}_{T_{ij}}^k\left[\mathbf{q}_{T_{ij}}^k + \left(\check{\mathbf{p}}_{T_{ij}}^k\right)^{-1}\check{\mathbf{x}}_{T_{ij}}^k\right]. \quad (23)$$

This is the case when static sensor networks with known positions are employed. However, as target j's state estimate has been used to update the robots' pose estimates in the localization part, its state estimate becomes correlated with the robots' pose estimates. Hence, here, we adopt the ICI (3) to fuse $(\check{\mathbf{p}}_{T_{ij}}^k, \check{\mathbf{x}}_{T_{ij}}^k)$ with $(\Omega_{T_{ij}}^k, \mathbf{q}_{T_{ij}}^k)$ to avoid information double-counting when the robots' pose estimates are, in turn, used in the relative correction pairs to compute the posterior estimate of target j. The proposed DEIF algorithm for target tracking is summarized in Tabel II.

Remark 3: In Table II, the prior estimates are weighted averaged over the communicating neighborhood. Therefore, a robot directly sensing target j can either directly or indirectly influence the other robots through the communication topology. Hence, target j's state is cooperatively estimated by each robot even if some robots cannot detect target j

TABLE II
DEIF ALGORITHM FOR TARGET TRACKING

Propagation:

$$\mathbf{\Phi}_{T_{ij}}^{k-1} = \frac{\partial\mathbf{g}_j}{\partial\mathbf{x}_{T_{ij}}}(\hat{\mathbf{x}}_{T_{ij}}^{k-1}), \qquad \mathbf{G}_{T_{ij}}^{k-1} = \frac{\partial\mathbf{g}_j}{\partial\mathbf{w}_{T_j}}(\hat{\mathbf{x}}_{T_{ij}}^{k-1}),$$
$$\mathbf{Q}_{T_{ij}}^{k-1} = \mathbf{G}_{T_{ij}}^{k-1}\mathbf{E}[\mathbf{w}_{T_j}^{k-1}(\mathbf{w}_{T_j}^{k-1})^\mathsf{T}](\mathbf{G}_{T_{ij}}^{k-1})^\mathsf{T},$$
$$\bar{\mathbf{p}}_{T_{ij}}^k = \mathbf{\Phi}_{T_{ij}}^{k-1}\mathbf{p}_{T_{ij}}^{k-1}(\mathbf{\Phi}_{T_{ij}}^{k-1})^\mathsf{T} + \mathbf{Q}_{T_{ij}}^{k-1},$$
$$\bar{\mathbf{x}}_{T_{ij}}^k = \mathbf{g}_j(\hat{\mathbf{x}}_{T_{ij}}^{k-1}).$$

Compute the update terms:

Obtain $(\check{\mathbf{p}}_{T_{ij}}^k, \check{\mathbf{x}}_{T_{ij}}^k)$ and $(\Omega_{T_{ij}}^k, \mathbf{q}_{T_{ij}}^k)$ using (19)-(22).
$$\mathbf{\Gamma}_{T_{ij}}^k = (\check{\mathbf{p}}_{T_{ij}}^k)^{-1}[\alpha_{ij}^k(\check{\mathbf{p}}_{T_{ij}}^k)^{-1} + (1-\alpha_{ij}^k)\Omega_{T_{ij}}^k]^{-1}\Omega_{T_{ij}}^k,$$
$$\mathbf{K}_{T_{ij}}^k = \Omega_{T_{ij}}^k - \alpha_{ij}^k\mathbf{\Gamma}_{T_{ij}}^k,$$
$$\mathbf{L}_{T_{ij}}^k = (\check{\mathbf{p}}_{T_{ij}}^k)^{-1} - (1-\alpha_{ij}^k)\mathbf{\Gamma}_{T_{ij}}^k.$$

Update:

$$\mathbf{p}_{T_{ij}}^k = [\Omega_{T_{ij}}^k + (\check{\mathbf{p}}_{T_{ij}}^k)^{-1} - \mathbf{\Gamma}_{T_{ij}}^k]^{-1}$$
$$\hat{\mathbf{x}}_{T_{ij}}^k = \mathbf{p}_{T_{ij}}^k[\mathbf{K}_{T_{ij}}^k(\Omega_{T_{ij}}^k)^{-1}\mathbf{q}_{T_{ij}}^k + \mathbf{L}_{T_{ij}}^k\check{\mathbf{x}}_{T_{ij}}^k].$$

The time-varying weight α_{ij}^k subject to $\alpha_{ij}^k \in [0,1]$ is selected to minimize $\mathrm{Tr}\{\mathbf{p}_{T_{ij}}^k\}$.

at a certain time. In addition, data association is required for multitarget tracking. However, it is out of the scope in this article. We assume that each robot knows exactly which measurement belongs to which target.

B. Joint Localization and Target Tracking

Based on Section III-A, we propose the JLATT algorithm from the DEIF perspective in a mobile robot network, where multiple relative measurements might take place at one robot, and each robot can communicate with its nearby neighbors within the communication range. We refer to the algorithm as JLATT-DEIF. It is worth noting that the communication and sensing topologies are subject to change with time and the robots not directly sensing the targets.

Initialization: For robot $i \in \mathcal{V}$, initialize the DEIF estimates $\mathbf{p}_{R_i}^0, \hat{\mathbf{x}}_{R_i}^0$ and $\mathbf{p}_{T_{ij}}^0, \hat{\mathbf{x}}_{T_{ij}}^0$, $\forall j \in \mathcal{U}$.
Propagation: As in Tables I and II.
Update:

1) Robot i obtains available relative measurements $\mathbf{z}_{R_{il}}^k$ to the other robots in $\mathcal{N}_{s,i}^k$ and $\mathbf{z}_{T_{ij}}^k$ to the targets. Recall that if target j is out of the sensing region of robot i, $(\bar{\mathbf{R}}_{T_{ij}}^k)^{-1} = 0$.
2) Robot i obtains its absolute measurement $\mathbf{z}_{R_i}^k$ if available and otherwise $(\mathbf{R}_{R_i}^k)^{-1} = 0$.
3) Receive $\{\bar{\mathbf{p}}_{T_{lj}}^k, \bar{\mathbf{x}}_{T_{lj}}^k, \tilde{\mathbf{s}}_{T_{lj}}^k, \tilde{\mathbf{y}}_{T_{lj}}^k\}$ from robot l, $\forall l \in \mathcal{N}_{c,i}^k$ and $\forall j \in \mathcal{U}$.
4) Compute localization correction pairs $\{\mathbf{s}_{R_{il}}^k, \mathbf{y}_{R_{il}}^k\}$, $\forall l \in \mathcal{N}_{s,i}^k$ as in (10) and (11), $\{\mathbf{s}_{T_{ij}}^k, \mathbf{y}_{T_{ij}}^k\}$, $\forall j \in \mathcal{U}_i^k$ as in (13) and (14) and $\{\mathbf{s}_{R_{ii}}^k, \mathbf{y}_{R_{ii}}^k\}$ as in (16).
5) Update the pose estimate of robot i as in Table I.
6) Compute tracking correction pairs $\{\tilde{\mathbf{s}}_{T_{ij}}^k, \tilde{\mathbf{y}}_{T_{ij}}^k\}$, $\forall j \in \mathcal{U}$ as in (19) and (20).

7) Update the state estimate of target $j \in \mathcal{U}$ as in Table II.

Remark 4: The state and covariance propagations and updates described in Tables I and II allow for a fully distributed JLATT-DEIF algorithm, which uses one-hop communication and requires no global parameter.

IV. STABILITY ANALYSIS

In this section, the stability of the proposed algorithm is analyzed in the linearized time-varying systems. By linearizing (6), the error propagation equation for robot i is given by

$$\bar{\mathbf{e}}_{R_i}^k = \Phi_{R_i}^{k-1}\mathbf{e}_{R_i}^{k-1} + \mathbf{G}_{R_i}^{k-1}\mathbf{w}_{R_i}^{k-1} \qquad (24)$$

where $\Phi_{R_i}^{k-1}$ and $\mathbf{G}_{R_i}^{k-1}$ are defined in Table I, with the measurement error equations given by (9), (12), and (15). By linearizing (7), the error propagation equation for target j is given by

$$\bar{\mathbf{e}}_{T_{ij}}^k = \Phi_{T_{ij}}^{k-1}\mathbf{e}_{T_{ij}}^{k-1} + \mathbf{G}_{T_{ij}}^{k-1}\mathbf{w}_{T_j}^{k-1} \qquad (25)$$

where $\Phi_{T_{ij}}^{k-1}$ and $\mathbf{G}_{T_{ij}}^{k-1}$ are defined in Table II, with the measurement error equation given by (12). We refer to (9), (12), (15), and (24) as the localization system and (25) and (12) as the tracking system, respectively. Furthermore, the motion, process, and measurement noise covariances are assumed to be time invariant for simplicity (i.e., $\mathbf{Q}_{R_i}^k = \mathbf{Q}_{R_i} > 0$, $\mathbf{Q}_{T_{ij}}^k = \mathbf{Q}_{T_{ij}} > 0$, $\mathbf{R}_{R_{ij}}^k = \mathbf{R}_{R_{ij}} > 0$, $\mathbf{R}_{R_i}^k = \mathbf{R}_{R_i} > 0$, and $\mathbf{R}_{T_{ij}}^k = \mathbf{R}_{T_{ij}} > 0$). Next, we focus on the localization part. We first give the definition of observable pairs.

Definition 2: The pair $(\mathbf{A}^\tau, \mathbf{C}^\tau)$, where τ is the time index, is observable on $\mathcal{T}_{j_0}^{j_1}$, if and only if the observability grammian

$$\sum_{\tau=j_0}^{j_1}[\mathbf{A}(\tau, j_0)]^\mathsf{T}(\mathbf{C}^\tau)^\mathsf{T}\mathbf{C}^\tau\mathbf{A}(\tau, j_0) > 0$$

where $\mathbf{A}(\tau, j_0)$ is the transition matrix on $\mathcal{T}_{j_0}^\tau$.

In order to evaluate the stability of the algorithm in Table I, we make the following assumptions.

Assumption 1: There exists a positive integer $\bar{k}$ such that at each time $k \geq \bar{k}$, the following statements hold.

1) There exists a nonempty subset $\mathcal{V}^k \subseteq \mathcal{V}$, such that for each robot $i \in \mathcal{V}^k$, the pair $(\Phi_{R_i}^\tau, \mathbf{C}_{R_i}^\tau)$ is observable on $\mathcal{T}_{k-\bar{k}}^{k-\bar{k}+\bar{n}}$, where $0 < \bar{n} < \bar{k}$.
2) For each robot $j \in \mathcal{V}\backslash\mathcal{V}^k$, there exists a directed path from a certain robot $i \in \mathcal{V}^k$ to j in the form of $(i_0, i_1), (i_1, i_2), \ldots, (i_{l-1}, i_l)$, where $i_0 = i$ and $i_l = j$, and l consecutive intervals of the form $\mathcal{T}_{m_0}^{m_1}, \ldots, \mathcal{T}_{m_{l-1}}^{m_l}$, where $m_0 = k - \bar{k} + \bar{n}$ and $m_l = k$, such that $(\Phi_{R_{i_s}}^\tau, \mathbf{H}_{R_{i_s i_{s-1}}}^\tau)$ is observable on $\mathcal{T}_{m_{s-1}}^{m_s}$, where $s = 1, \ldots, l$.

Assumption 2: For each $k \geq 0$ and each robot $i \in \mathcal{V}$, the system matrix $\Phi_{R_i}^k$ is invertible.

Assumption 3: For each robot $i \in \mathcal{V}$, the initialized estimation pair $(\hat{\mathbf{x}}_{R_i}^0, \mathbf{p}_{R_i}^0)$ is consistent. That is,

$$\mathbb{E}\{\mathbf{e}_{R_i}^0(\mathbf{e}_{R_i}^0)^\mathsf{T}\} \leq \mathbf{p}_{R_i}^0.$$

Remark 5: As for Assumption 1, $\mathcal{V}^k$ can be changing over time. For example, $\mathcal{V}^k$ might just contain one robot at times. Furthermore, none of the robots needs to receive absolute measurements on $\mathcal{T}_{m_0}^k$. In other words, for either absolute or relative measurements, only a sparse possibly changing subset of the team needs to have access to, and those measurements can be intermittent. Assumption 2 is automatically satisfied as $\Phi_{R_i}^k$ is obtained by the discretization of a continuous-time system before linearization. Finally, Assumption 3 can be guaranteed by initializing $\mathbf{p}_{R_i}^0$ with a sufficiently large value.

Next, we give the main stability result of the localization part and then prove it step by step.

Theorem 1: Suppose that Assumptions 1–3 hold. Then, the pose estimate of each robot is stable under the algorithm in Table I. That is, for each robot $i \in \mathcal{V}$, there exists a positive definite matrix $\mathbf{p}_i$ such that

$$\mathbb{E}\{\mathbf{e}_{R_i}^k(\mathbf{e}_{R_i}^k)^\mathsf{T}\} \leq \mathbf{p}_i$$

for any $k \geq \bar{k}$.

In order to prove the above stability result, we first study the consistency of the estimates.

Lemma 2: Let Assumption 3 hold. For each robot $i \in \mathcal{V}$, the estimation pair $(\hat{\mathbf{x}}_{R_i}^k, \mathbf{p}_{R_i}^k)$ obtained from the proposed DEIF in Table I is consistent, that is,

$$\mathbb{E}\{\mathbf{e}_{R_i}^k(\mathbf{e}_{R_i}^k)^\mathsf{T}\} \leq \mathbf{p}_{R_i}^k \quad \forall k \geq 0.$$

Proof: The proof is shown by induction. When $k = 0$, Assumption 3 implies that $\mathbb{E}\{\mathbf{e}_{R_i}^0(\mathbf{e}_{R_i}^0)^\mathsf{T}\} \leq \mathbf{p}_{R_i}^0$. Then, it is assumed that at time $k - 1$, $\mathbb{E}\{\mathbf{e}_{R_i}^{k-1}(\mathbf{e}_{R_i}^{k-1})^\mathsf{T}\} \leq \mathbf{p}_{R_i}^{k-1}$. Notice that the propagation error satisfies

$$\bar{\mathbf{e}}_{R_i}^k = \Phi_{R_i}^{k-1}\mathbf{e}_{R_i}^{k-1} + \mathbf{G}_{R_i}^{k-1}\mathbf{w}_{R_i}^{k-1}.$$

Because $\mathbb{E}\{\bar{\mathbf{e}}_{R_i}^k(\mathbf{w}_{R_i}^k)^\mathsf{T}\} = 0$, it follows that:

$$\begin{aligned}\mathbb{E}\{\bar{\mathbf{e}}_{R_i}^k(\bar{\mathbf{e}}_{R_i}^k)^\mathsf{T}\} &= \Phi_{R_i}^{k-1}\mathbb{E}\{\mathbf{e}_{R_i}^{k-1}(\mathbf{e}_{R_i}^{k-1})^\mathsf{T}\}(\Phi_{R_i}^{k-1})^\mathsf{T} + \mathbf{Q}_{R_i} \\ &\leq \Phi_{R_i}^{k-1}\mathbf{p}_{R_i}^{k-1}(\Phi_{R_i}^{k-1})^\mathsf{T} + \mathbf{Q}_{R_i} = \bar{\mathbf{p}}_{R_i}^k.\end{aligned}$$

Next, as analyzed in Section III-A, by exploiting the consistency property of ICI, the update step in Table I is guaranteed to be consistent. It follows that $\mathbb{E}\{\mathbf{e}_{R_i}^k(\mathbf{e}_{R_i}^k)^\mathsf{T}\} \leq \mathbf{p}_{R_i}^k$. $\quad\square$

Lemma 2 points out that, in order to prove the boundedness of the actual error covariance, it is sufficient to show that the estimated covariance $\mathbf{p}_{R_i}^k$ is upper bounded by a certain constant matrix.

Lemma 3 [13]: Let Φ be a nonsingular matrix. For any $\mathbf{Q} > 0$ and $\check{\mathbf{p}} > 0$, there exists a parameter $\beta \in (0, 1]$ such that $(\Phi\mathbf{p}\Phi^\mathsf{T} + \mathbf{Q})^{-1} \geq \beta\Phi^{-\mathsf{T}}\mathbf{p}^{-1}\Phi^{-1}$ for any $\mathbf{p} \geq \check{\mathbf{p}}$.

Lemma 4: Suppose that Assumptions 1–3 hold. Then, for each $i \in \mathcal{V}$, there exists a positive-definite matrix $\mathbf{p}_i$ such that

$$\mathbf{p}_{R_i}^k \leq \mathbf{p}_i \quad \forall k \geq \bar{k}.$$

Proof: To simplify the notation, for certain time τ and τ_0, we define $\tilde{\tau}_{\tau_0} = \tau - \tau_0$. First, we focus on robot $i \in \mathcal{V}^k$. At any time $a \in \mathcal{T}_{m_0}^k$, the inverse of the updated covariance can be written as

$$(\mathbf{p}_{R_i}^a)^{-1} = \Omega_{R_i}^a + \sum_{l \in \mathcal{N}_{s,i}^a}\eta_{il}^a\mathbf{s}_{R_{il}}^a + \sum_{j \in \mathcal{U}_i^a}\eta_{ij}^a\mathbf{s}_{T_{ij}}^a + \mathbf{s}_{R_{ii}}^a - \Gamma_{R_i}^a.$$

Invoking Lemma 1, one can get the lower bound

$$
\begin{aligned}
\left(\mathbf{p}_{R_i}^a\right)^{-1} &\geq \alpha_a \Omega_{R_i}^a + (1-\alpha_a)\left(\sum_{l\in\mathcal{N}_{s,i}^a} \eta_{il}^a \mathbf{s}_{R_{il}}^a + \mathbf{s}_{R_{ii}}^a\right) \\
&= \alpha_a \Psi\left\{\left(\mathbf{p}_{R_i}^{a-1}\right)^{-1}\right\} + (1-\alpha_a)\left(\sum_{l\in\mathcal{N}_{s,i}^a} \eta_{il}^a \mathbf{s}_{R_{il}}^a + \mathbf{s}_{R_{ii}}^a\right)
\end{aligned}
$$

where $\Psi\{(\mathbf{p}_{R_i}^{a-1})^{-1}\} = [\Phi_{R_i}^{a-1}\mathbf{p}_{R_i}^{a-1}(\Phi_{R_i}^{a-1})^{\mathsf{T}} + \mathbf{Q}_{R_i}]^{-1}$ and $\alpha_a \in (0,1)$. Furthermore, under Assumption 2, it follows from Lemma 3 that:

$$
\Psi\left\{\left(\mathbf{p}_{R_i}^{a-1}\right)^{-1}\right\} \geq \beta_a \left(\Phi_{R_i}^{a-1}\right)^{-\mathsf{T}}\left(\mathbf{p}_{R_i}^{a-1}\right)^{-1}\left(\Phi_{R_i}^{a-1}\right)^{-1}
$$

with $\beta_a \in (0,1]$, for any $\mathbf{p}_{R_i}^{a-1} \geq \mathbb{E}\{\mathbf{e}_{R_i}^{a-1}(\mathbf{e}_{R_i}^{a-1})^{\mathsf{T}}\}$. Then, one can obtain

$$
\begin{aligned}
\left(\mathbf{p}_{R_i}^a\right)^{-1} &\geq \alpha_a \beta_a \left(\Phi_{R_i}^{a-1}\right)^{-\mathsf{T}}\left(\mathbf{p}_{R_i}^{a-1}\right)^{-1}\left(\Phi_{R_i}^{a-1}\right)^{-1} \\
&\quad + (1-\alpha_a)\left(\sum_{l\in\mathcal{N}_{s,i}^a} \eta_{il}^a \mathbf{s}_{R_{il}}^a + \mathbf{s}_{R_{ii}}^a\right). \quad (26)
\end{aligned}
$$

where we can further write

$$
\begin{aligned}
\left(\mathbf{p}_{R_i}^{a-1}\right)^{-1} &\geq \alpha_{a-1}\beta_{a-1}\left(\Phi_{R_i}^{a-2}\right)^{-\mathsf{T}}\left(\mathbf{p}_{R_i}^{a-2}\right)^{-1}\left(\Phi_{R_i}^{a-2}\right)^{-1} \\
&\quad + (1-\alpha_{a-1})\left(\sum_{l\in\mathcal{N}_{s,i}^{a-1}} \eta_{il}^{a-1} \mathbf{s}_{R_{il}}^{a-1} + \mathbf{s}_{R_{ii}}^{a-1}\right). \quad (27)
\end{aligned}
$$

By recursively substituting (27) into (26) for $\bar{a} = a - \tilde{k}_{\bar{k}}$ times, one can write

$$
\left(\mathbf{p}_{R_i}^a\right)^{-1} \geq \sum_{\tau=0}^{\bar{a}} \check{\alpha}_\tau \check{\beta}_\tau \Phi_{R_i}^{-\mathsf{T}}(a,\tilde{a}_\tau)\triangle\Phi_{R_i}^{-1}(a,\tilde{a}_\tau) \quad (28)
$$

where $\Phi_{R_i}(a,\tilde{a}_\tau)$ is the transition matrix on $\mathcal{T}_a^{\tilde{a}_\tau}$, $\triangle = \sum_{l\in\mathcal{N}_{s,i}^{\tilde{a}_\tau}} \eta_{il}^{\tilde{a}_\tau} \mathbf{s}_{R_{il}}^{\tilde{a}_\tau} + \mathbf{s}_{R_{ii}}^{\tilde{a}_\tau}$, $\check{\alpha}_\tau = (1-\alpha_{\tilde{a}_\tau})\prod_{j=0}^{\tau-1}\alpha_{\tilde{a}_j}$ and $\check{\beta}_\tau = \prod_{j=0}^{\tau-1}\beta_{\tilde{a}_j}$, for $\tau > 0$, and $\check{\alpha}_\tau = (1-\alpha_a)$ and $\check{\beta}_\tau = 1$, for $\tau = 0$. Note that the right-hand side of (28) can be equivalently written as $\Phi_{R_i}^{-\mathsf{T}}(a,\tilde{a}_{\bar{a}})\Psi\Phi_{R_i}^{-1}(a,\tilde{a}_{\bar{a}})$, where

$$
\begin{aligned}
\Psi &= \sum_{\tau=0}^{\bar{a}} \check{\alpha}_\tau \check{\beta}_\tau \Phi_{R_i}^{\mathsf{T}}(\tilde{a}_\tau,\tilde{a}_{\bar{a}})\triangle\Phi_{R_i}(\tilde{a}_\tau,\tilde{a}_{\bar{a}}) \\
&= \sum_{\tau=0}^{\bar{a}-\bar{n}-1} \check{\alpha}_\tau \check{\beta}_\tau \Phi_{R_i}^{\mathsf{T}}(\tilde{a}_\tau,\tilde{a}_{\bar{a}})\triangle\Phi_{R_i}(\tilde{a}_\tau,\tilde{a}_{\bar{a}}) \\
&\quad + \sum_{\tau=\bar{a}-\bar{n}}^{\bar{a}} \check{\alpha}_\tau \check{\beta}_\tau \Phi_{R_i}^{\mathsf{T}}(\tilde{a}_\tau,\tilde{a}_{\bar{a}})\triangle\Phi_{R_i}(\tilde{a}_\tau,\tilde{a}_{\bar{a}}).
\end{aligned}
$$

Invoking part (1) of Assumption 1, $(\Phi_{R_i}^\tau, \mathbf{C}_{R_i}^\tau)$ is observable on $\mathcal{T}_{a-\bar{a}}^{a-\bar{a}+\bar{n}}$. We have

$$
\sum_{\tau=\bar{a}-\bar{n}}^{\bar{a}} \Phi_{R_i}^{\mathsf{T}}(\tilde{a}_\tau,\tilde{a}_{\bar{a}})(\mathbf{C}_{R_i}^{\tilde{a}_\tau})^{\mathsf{T}}\mathbf{C}_{R_i}^{\tilde{a}_\tau}\Phi_{R_i}(\tilde{a}_\tau,\tilde{a}_{\bar{a}}) > 0.
$$

Recall that $\mathbf{s}_{R_{ii}}^\tau = (\mathbf{C}_{R_i}^k)^{\mathsf{T}}\mathbf{R}_{R_i}^{-1}\mathbf{C}_{R_i}^k$. Then, by noticing that $\check{\alpha}_\tau \in (0,1)$, $\check{\beta}_\tau \in (0,1]$ and $\mathbf{R}_{R_i}^{-1} > 0$, it can be seen that

$$
\Psi \geq \sum_{\tau=\bar{a}-\bar{n}}^{\bar{a}} \check{\alpha}_\tau \check{\beta}_\tau \Phi_{R_i}^{\mathsf{T}}(\tilde{a}_\tau,\tilde{a}_{\bar{a}})\mathbf{s}_{R_{ii}}^{\tilde{a}_\tau}\Phi_{R_i}(\tilde{a}_\tau,\tilde{a}_{\bar{a}}) > 0.
$$

Hence, we can obtain a positive-definite matrix

$$
\left(\mathbf{p}_i^a\right)^{-1} = \sum_{\tau=\bar{a}-\bar{n}}^{\bar{a}} \check{\alpha}_\tau \check{\beta}_\tau \Phi_{R_i}^{-\mathsf{T}}(a,\tilde{a}_\tau)\mathbf{s}_{R_{ii}}^{\tilde{a}_\tau}\Phi_{R_i}^{-1}(a,\tilde{a}_\tau)
$$

such that $\mathbf{p}_{R_i}^a \leq \mathbf{p}_i^a$. Furthermore, let $\bar{\mathbf{p}}_i = \Phi_{R_i}\mathbf{p}_i(\Phi_{R_i})^{\mathsf{T}} + \mathbf{Q}_{R_i}$, where $\Phi_{R_i} \geq \Phi_{R_i}^\tau$, $\forall\tau \in \mathcal{T}_{k-\bar{k}}^a$. We have $\bar{\mathbf{p}}_{R_i}^k \leq \bar{\mathbf{p}}_i^a$. As a is arbitrary in $\mathcal{T}_{m_0}^k$, it follows that there exist, respectively, positive matrices $\mathbf{p}_i$ and $\bar{\mathbf{p}}_i$ such that $\mathbf{p}_{R_i}^\tau \leq \mathbf{p}_i$, $\bar{\mathbf{p}}_{R_i}^\tau \leq \bar{\mathbf{p}}_i$ and $\forall\tau \in \mathcal{T}_{m_0}^k$.

Next, consider the robots in $\mathcal{V}\backslash\mathcal{V}^k$. Starting from robot j to which there exists an edge from one robot $i \in \mathcal{V}^k$ on $\mathcal{T}_{m_0}^{m_1}$. Such robot j exists due to part (2) of Assumption 1. Following a similar process, at any time $b \in \mathcal{T}_{m_1}^k$, after $\bar{b} = b - m_0$ iterations, one can obtain

$$
\left(\mathbf{p}_{R_j}^b\right)^{-1} \geq \sum_{\tau=\bar{b}-\bar{m}_1}^{\bar{b}} \check{\alpha}_\tau \check{\beta}_\tau \Phi_{R_j}^{-\mathsf{T}}(b,\tilde{b}_\tau)\left(\sum_{l\in\mathcal{N}_{s,j}^{\tilde{b}_\tau}} \eta_{jl}^{\tilde{b}_\tau} \mathbf{s}_{R_{jl}}^{\tilde{b}_\tau}\right)\Phi_{R_j}^{-1}(b,\tilde{b}_\tau)
$$

where $\Phi_{R_j}(b,\tilde{b}_\tau)$ is the transition matrix on $\mathcal{T}_b^{\tilde{b}_\tau}$, and $\bar{m}_1 = m_1 - m_0$. Note that it is possible that $\mathbf{s}_{R_{jj}}^\tau = 0$, $\forall\tau \in \mathcal{T}_{k-\bar{k}}^k$ but $\mathcal{N}_{s,j}^\tau$ contains i on $\mathcal{T}_{m_0}^{m_1}$. Then, one can write

$$
\left(\mathbf{p}_{R_j}^b\right)^{-1} \geq \sum_{\tau=\bar{b}-\bar{m}_1}^{\bar{b}} \check{\alpha}_\tau \check{\beta}_\tau \Phi_{R_j}^{-\mathsf{T}}(b,\tilde{b}_\tau)\eta_{ji}^{\tilde{b}_\tau}\mathbf{s}_{R_{ji}}^{\tilde{b}_\tau}\Phi_{R_j}^{-1}(b,\tilde{b}_\tau).
$$

Recall from (10) and (11) that

$$
\begin{aligned}
\mathbf{s}_{R_{ji}}^\tau &= \left(\mathbf{H}_{R_{ji}}^\tau\right)^{\mathsf{T}}\left(\bar{\mathbf{R}}_{R_{ji}}^\tau\right)^{-1}\mathbf{H}_{R_{ji}}^\tau \\
&= \left(\mathbf{H}_{R_{ji}}^\tau\right)^{\mathsf{T}}\left\{\mathbf{R}_{R_{ji}} + \widetilde{\mathbf{H}}_{R_{ji}}^\tau\bar{\mathbf{p}}_{R_i}^\tau\left(\widetilde{\mathbf{H}}_{R_{ji}}^\tau\right)^{\mathsf{T}}\right\}^{-1}\mathbf{H}_{R_{ji}}^\tau.
\end{aligned}
$$

It can be immediately seen that the boundedness of $\mathbf{p}_{R_j}^\tau$ is related to $\bar{\mathbf{p}}_{R_i}^\tau$. As $\bar{\mathbf{p}}_{R_i}^\tau \leq \bar{\mathbf{p}}_i$, there exists $\widetilde{\mathbf{H}}_{R_{ji}} \in \{\widetilde{\mathbf{H}}_{R_{ji}}^\tau \mid \tau \in \mathcal{T}_{m_0}^{m_1}\}$ such that $\bar{\mathbf{R}}_{R_{ji}}^\tau \leq \bar{\mathbf{R}}_{R_{ji}} = \mathbf{R}_{R_{ji}} + \widetilde{\mathbf{H}}_{R_{ji}}\bar{\mathbf{p}}_i(\widetilde{\mathbf{H}}_{R_{ji}})^{\mathsf{T}}$, $\forall\tau \in \mathcal{T}_{m_0}^{m_1}$. Then, we can write $\mathbf{s}_{R_{ji}}^\tau \geq \underline{\mathbf{s}}_{R_{ji}}^\tau > 0$, where $\underline{\mathbf{s}}_{R_{ji}}^\tau = (\mathbf{H}_{R_{ji}}^\tau)^{\mathsf{T}}(\bar{\mathbf{R}}_{R_{ji}})^{-1}\mathbf{H}_{R_{ji}}^\tau$, $\forall\tau \in \mathcal{T}_{m_0}^{m_1}$. Invoking part (2) in Assumption 1, $(\Phi_{R_j}^\tau, \mathbf{H}_{R_{ji}}^\tau)$ is observable on $\mathcal{T}_{b-\bar{b}}^{b-\bar{b}+\bar{m}_1}$. We have

$$
\sum_{\tau=\bar{b}-\bar{m}_1}^{\bar{b}} \Phi_{R_j}^{\mathsf{T}}(\tilde{b}_\tau,\tilde{b}_{\bar{b}})(\mathbf{H}_{R_{ji}}^{\tilde{b}_\tau})^{\mathsf{T}}\mathbf{H}_{R_{ji}}^{\tilde{b}_\tau}\Phi_{R_j}(\tilde{b}_\tau,\tilde{b}_{\bar{b}}) > 0.
$$

Then, by noticing that $\check{\alpha}_\tau \in (0,1)$, $\check{\beta}_\tau \in (0,1]$, $\eta_{ji}^{\tilde{b}_\tau} \in (0,1]$ and $\bar{\mathbf{R}}_{R_{ji}}^{-1} > 0$, we can obtain a positive-definite matrix

$$
\left(\mathbf{p}_j^b\right)^{-1} = \sum_{\tau=\bar{b}-\bar{m}_1}^{\bar{b}} \check{\alpha}_\tau \check{\beta}_\tau \eta_{ji}^{\tilde{b}_\tau}\Phi_{R_j}^{-\mathsf{T}}(b,\tilde{b}_\tau)\underline{\mathbf{s}}_{R_{ji}}^{\tilde{b}_\tau}\Phi_{R_j}^{-1}(b,\tilde{b}_\tau)
$$

such that $\mathbf{p}_{R_j}^b \leq \mathbf{p}_j^b$. Hence, we can claim that there exists a matrix $\mathbf{p}_j$ such that $\mathbf{p}_{R_j}^\tau \leq \mathbf{p}_j$, $\forall\tau \in \mathcal{T}_{m_1}^k$. In addition, we can find an upper bound $\bar{\mathbf{p}}_j$ of $\bar{\mathbf{p}}_{R_j}^\tau$, where $\tau \in \mathcal{T}_{m_1}^k$.

Similarly, for another robot $l \in \mathcal{V}\backslash\mathcal{V}^k$ to which there exists an edge from robot j on $\mathcal{T}_{m_1}^{m_2}$. We can obtain a positive-definite matrix $\mathbf{p}_l$ which is associated with $\bar{\mathbf{p}}_j$, such that $\mathbf{p}_{R_l}^\tau \leq \mathbf{p}_l$, $\forall\tau \in \mathcal{T}_{m_2}^k$.

Part (2) of Assumption 1 says that for each robot in $\mathcal{V}\backslash\mathcal{V}^k$, there exists a directed path from one robot in $\mathcal{V}^k$ to that robot.

By applying the above-mentioned approach orderly along that directed path, it takes $\bar{k}-\bar{n}$ time instants to make the estimated pose covariance of the farthest robot upper bounded, where $\bar{k}-\bar{n}$ is the total length of l consecutive intervals. As this is the case for any $k \geq \bar{k}$, we can conclude the proof. $\qquad\square$

Hence, the statement of Theorem 1 follows directly from Lemmas 2 and 4.

Since the stability analysis is the same for each target, we focus on one target $j \in \mathcal{U}$. Furthermore, as the proof follows a similar approach to that of Theorem 1, only the different parts are shown in detail in the following. We first give the definition of the observable joint set and orderly appearing path as follows.

Definition 3: Let $\mathcal{V}'$ be a nonempty subset of $\mathcal{V}$. The tracking system (12) and (25) of target j is jointly observable to the robots in $\mathcal{V}'$ on $\mathcal{T}_{j_0}^{j_1}$ if and only if the joint observability grammian

$$\sum_{l \in \mathcal{V}'} \sum_{\tau=j_0}^{j_1} [\Phi_{T_{lj}}(\tau, j_0)]^{\mathsf{T}} (\widetilde{\mathbf{H}}_{T_{lj}}^{\tau})^{\mathsf{T}} \widetilde{\mathbf{H}}_{T_{lj}}^{\tau} \Phi_{T_{lj}}(\tau, j_0) > 0$$

where $\Phi_{T_{lj}}(\tau, j_0)$ is the transition matrix on $\mathcal{T}_{\tau_0}^{\tau}$.

Definition 4 [31]: Let $\mathcal{B} = \{e_1, \ldots, e_p\}$, where $e_j = (i_{j-1}, i_j)$, $\forall j = 1, \ldots, p$, be a direct path in a graph. Then, $\mathcal{B}$ is an orderly appearing path on $\mathcal{T}_{\tau_0}^{\tau_1}$, if there exist p time instants $\tau_{l_1} < \tau_{l_2} < \ldots, < \tau_{l_p}$ on $\mathcal{T}_{\tau_0}^{\tau_1}$ such that e_j is an edge (including the self-edge) of that graph at time τ_{l_i}, where $i = 1, \ldots, p$.[1]

In order to derive the stability result of the algorithm in Table II, the following assumptions and a lemma are needed.

Assumption 4: There exists a positive integer $\bar{l}$, such that for each robot $i \in \mathcal{V}$ at each time $k \geq \bar{k} + \bar{l}$, where $\bar{k}$ is from Assumption 1, one can find a nonempty robot subset $\mathcal{V}_i^k \subseteq \mathcal{V}$ that satisfies the following statements.

1) $\mathcal{V}_i^k$ has joint observability about target j on $\mathcal{T}_{k-\bar{l}}^{k-\bar{l}+\bar{m}}$, where $0 < \bar{m} < \bar{l}$.
2) Every robot in $\mathcal{V}_i^k$ has an orderly appearing path in the communication graph G_c^{τ} to i on $\mathcal{T}_{k-\bar{l}+\bar{m}}^k$.

Assumption 5: For any $k \geq 0$, the system matrix $\Phi_{T_{lj}}^k$ is invertible.

Assumption 6: For each robot $i \in \mathcal{V}$, the initialized estimation pair $(\hat{\mathbf{x}}_{T_{ij}}^0, \mathbf{p}_{T_{ij}}^0)$ is consistent. That is

$$\mathbb{E}\{\mathbf{e}_{T_{ij}}^0 (\mathbf{e}_{T_{ij}}^0)^{\mathsf{T}}\} \leq \mathbf{p}_{T_j}^0.$$

Let $\mathbf{D}^k = [\mathbf{D}_{il}^k]$ be the stochastic adjacently matrix associated with G_c^k at time k, where $\mathbf{D}_{il}^k = \pi_{il}^k$ with $\pi_{il}^k \in (0, 1]$ being the weights from the algorithm in Table II if $l \in \mathcal{J}_{c,i}^k$ and $\mathbf{D}_{il}^k = 0$ otherwise.

Lemma 5 [31]: Given a finite-time interval $\mathcal{T}_{j_0}^{j_1}$, let $\mathcal{D}_{j_0}^{j_1} = \mathbf{D}^{j_1}, \ldots, \mathbf{D}^{j_0+1} \mathbf{D}^{j_0}$. Then, $\{\mathcal{D}_{j_0}^{j_1}\}_{il} > 0$ if and only if there exists an orderly appearing path from i to l on $\mathcal{T}_{j_0}^{j_1}$.

The following theorem shows the stability result of the tracking part.

Theorem 2: Suppose that Assumptions 1–6 hold. Then, target j's state estimate obtained by each robot is stable under

the algorithm in Table II. That is, for each $i \in \mathcal{V}$, there exists a positive-definite matrix $\mathbf{p}_{i,j}$ such that

$$\mathbb{E}\{\mathbf{e}_{T_{ij}}^k (\mathbf{e}_{T_{ij}}^k)^{\mathsf{T}}\} \leq \mathbf{p}_{i,j}$$

for each $k \geq \bar{k} + \bar{l}$.

Proof: Notice that the consistency of the update step is preserved by ICI, as shown in Section III-A2. Then, under Assumption 6, following the same process as in Lemma 2, we can get the consistency result. That is, for each robot $i \in \mathcal{V}$

$$\mathbb{E}\{\mathbf{e}_{T_{ij}}^{\tau} (\mathbf{e}_{T_{ij}}^{\tau})^{\mathsf{T}}\} \leq \mathbf{p}_{T_{ij}}^{\tau} \quad \forall \tau \geq 0.$$

As Assumption 5 holds, for each robot $i \in \mathcal{V}$ at time k, where $k \geq \bar{k} + \bar{l}$, by following a similar approach to that in Lemma 4, we have:

$$(\mathbf{p}_{T_{ij}}^k)^{-1} \geq \sum_{l \in \mathcal{V}} \alpha_k \beta_k (\Phi_{T_{lj}}^{k-1})^{-\mathsf{T}} \mathbf{D}_{il}^k (\mathbf{p}_{T_{ij}}^{k-1})^{-1} (\Phi_{T_{lj}}^{k-1})^{-1}$$
$$+ (1 - \alpha_k) \sum_{l \in \mathcal{J}_{c,i}^k} \tilde{\eta}_{lj}^k \tilde{\mathbf{s}}_{T_{lj}}^k$$

where $\alpha_k \in (0, 1)$ and $\beta_k \in (0, 1]$. Then, by noticing that $\sum_{l \in \mathcal{J}_{c,i}^k} \tilde{\mathbf{s}}_{T_{lj}}^k \geq \sum_{l \in \mathcal{V}} \mathbf{D}_{il}^k \tilde{\mathbf{s}}_{T_{lj}}^k$, after $\bar{l}$ iterations, one can write

$$(\mathbf{p}_{T_{ij}}^k)^{-1} \geq \sum_{\tau=\bar{l}-\bar{m}}^{\bar{l}} \check{\alpha}_{\tau} \check{\beta}_{\tau} \sum_{l \in \mathcal{V}} \Phi_{T_{lj}}^{-\mathsf{T}}(k, \tilde{k}_{\tau})$$
$$\times \{\mathcal{D}_{k-\tau}^k\}_{il} \tilde{\eta}_{lj}^{\tilde{k}_{\tau}} \tilde{\mathbf{s}}_{T_{lj}}^{\tilde{k}_{\tau}} \Phi_{T_{lj}}^{-1}(k, \tilde{k}_{\tau}) \quad (29)$$

where $\check{\alpha}_{\tau} = (1 - \alpha_{\tilde{a}_{\tau}}) \prod_{j=0}^{\tau-1} \alpha_{\tilde{a}_j}$ and $\check{\beta}_{\tau} = \prod_{j=0}^{\tau-1} \beta_{\tilde{a}_j}$, for $\tau > 0$, and $\check{\alpha}_{\tau} = 1 - \alpha_a$ and $\check{\beta}_{\tau} = 1$, for $\tau = 0$. Equation (29) can be further written as

$$(\mathbf{p}_{T_{ij}}^k)^{-1} \geq \sum_{l \in \mathcal{V}} \Phi_{T_{lj}}^{-\mathsf{T}}(k, \tilde{k}_{\bar{k}})$$
$$\times \left[\sum_{\tau=\bar{l}-\bar{m}}^{\bar{l}} \check{\alpha}_{\tau} \check{\beta}_{\tau} \Phi_{T_{lj}}^{\mathsf{T}}(\tilde{k}_{\tau}, \tilde{k}_{\bar{k}}) \right.$$
$$\left. \times \{\mathcal{D}_{\tilde{k}_{\tau}}^k\}_{il} \tilde{\eta}_{lj}^{\tilde{k}_{\tau}} \tilde{\mathbf{s}}_{T_{lj}}^{\tilde{k}_{\tau}} \Phi_{T_{lj}}(\tilde{k}_{\tau}, \tilde{k}_{\bar{k}}) \right] \Phi_{T_{lj}}^{-1}(k, \tilde{k}_{\bar{k}}).$$

As part (2) of Assumption 4 is satisfied, it follows from Lemma 5 that $\{\mathcal{D}_{\tilde{k}_{\tau}}^k\}_{il} > 0$, $\forall l \in \mathcal{V}_i^k$ and $\forall \tau \in \mathcal{T}_{\bar{l}-\bar{m}}^{\bar{l}}$. Then, from part (1) of Assumption 4, we can claim that

$$\sum_{l \in \mathcal{V}} \sum_{\tau=\bar{l}-\bar{m}}^{\bar{l}} \Phi_{T_{lj}}^{\mathsf{T}}(\tilde{k}_{\tau}, \tilde{k}_{\bar{k}}) \{\mathcal{D}_{\tilde{k}_{\tau}}^k\}_{il} (\widetilde{\mathbf{H}}_{T_{lj}}^{\tilde{k}_{\tau}})^{\mathsf{T}} \widetilde{\mathbf{H}}_{T_{lj}}^{\tilde{k}_{\tau}} \Phi_{T_{lj}}(\tilde{k}_{\tau}, \tilde{k}_{\bar{k}})$$

is positive definite. Recall from (13) and (14) that

$$\tilde{\mathbf{s}}_{T_{lj}}^{\tau} = (\widetilde{\mathbf{H}}_{T_{lj}}^{\tau})^{\mathsf{T}} (\bar{\mathbf{R}}_{T_{lj}}^{\tau})^{-1} \widetilde{\mathbf{H}}_{T_{lj}}^{\tau}$$
$$= (\widetilde{\mathbf{H}}_{T_{lj}}^{\tau})^{\mathsf{T}} \left\{ \mathbf{R}_{T_{lj}} + \mathbf{H}_{T_{lj}}^{\tau} \bar{\mathbf{p}}_{R_l}^{\tau} (\mathbf{H}_{T_{lj}}^{\tau})^{\mathsf{T}} \right\}^{-1} \widetilde{\mathbf{H}}_{T_{lj}}^{\tau}.$$

Invoking Theorem 1, for any $\tau \geq \bar{k}$, there exists an upper bound $\bar{\mathbf{p}}_l$ for $\bar{\mathbf{p}}_{R_l}^{\tau}$, $\forall l \in \mathcal{V}$. Then, there exists $\mathbf{H}_{T_{lj}} \in \{\mathbf{H}_{T_{lj}}^{\tau} \mid \tau \in \mathcal{T}_{k-\bar{l}}^{k-\bar{l}+\bar{m}}\}$ such that $\bar{\mathbf{R}}_{T_{lj}}^{\tau} \leq \bar{\mathbf{R}}_{T_{lj}} = \mathbf{R}_{T_{lj}} + \mathbf{H}_{T_{lj}} \bar{\mathbf{p}}_l (\mathbf{H}_{T_{lj}})^{\mathsf{T}}$, $\forall \tau \in \mathcal{T}_{k-\bar{l}}^{k-\bar{l}+\bar{m}}$. Then, we can write $\tilde{\mathbf{s}}_{T_{lj}}^{\tau} \geq \underline{\tilde{\mathbf{s}}}_{T_{lj}}^{\tau}$, where $\underline{\tilde{\mathbf{s}}}_{T_{lj}}^{\tau} =$

---

[1]By default (i, i) itself can be an orderly appearing path.

$(\widetilde{\mathbf{H}}_{T_{lj}}^{\tau})^{\mathsf{T}}\bar{\mathbf{R}}_{T_{lj}}^{-1}\widetilde{\mathbf{H}}_{T_{lj}}^{\tau}$, $\forall \tau \in \mathcal{T}_{k-\bar{l}}^{k-\bar{l}+\bar{m}}$. Let $\mathcal{B}^{\tau} \subseteq \mathcal{V}$ be the set of blind robots at time τ. On $\mathcal{T}_{k-\bar{l}}^{k-\bar{l}+\bar{m}}$, as $\mathcal{V}_i^{\tau}$ is nonempty, $\mathcal{V}\backslash\mathcal{B}^{\tau}$ (the set of robots directly detects target j) is nonempty. For any $l \in \mathcal{V}\backslash\mathcal{B}^{\tau}$, we have $\tilde{\eta}_{lj}^{\tau} \in (0, 1]$ and $\mathbf{R}_{T_{lj}}^{-1} > 0$, $\forall \tau \in \mathcal{T}_{k-\bar{l}}^{k-\bar{l}+\bar{m}}$. Furthermore, by noticing that $\breve{\alpha}_{\tau} \in (0, 1)$, $\breve{\beta}_{\tau} \in (0, 1]$ and $\mathcal{V}_i^{\tau} \subseteq \mathcal{V}\backslash\mathcal{B}^{\tau}$, we can obtain a positive-definite matrix $(\mathbf{p}_{i,j})^{-1}$ as

$$\sum_{l \in \mathcal{V}} \sum_{\tau=\bar{l}-\bar{m}}^{\bar{l}} \breve{\alpha}_{\tau}\breve{\beta}_{\tau}\tilde{\eta}_{lj}^{\tilde{k}_{\tau}} \Phi_{T_{lj}}^{-\mathsf{T}}(k, \tilde{k}_{\tau})\{\mathcal{D}_{\tilde{k}_{\tau}}^k\}_{il}\tilde{\mathbf{s}}_{T_{lj}}^{\tilde{k}_{\tau}} \Phi_{T_{lj}}^{-1}(k, \tilde{k}_{\tau})$$

such that $\mathbf{p}_{T_{ij}}^k \leq \mathbf{p}_{i,j}$.

Hence, the proof can be concluded by noticing that in the above proof, i is arbitrary chosen from $\mathcal{V}$ for each time $k \geq \bar{k} + \bar{l}$. $\square$

V. SIMULATION

In this section, the performance of the proposed JLATT-DEIF algorithm is tested via a series of Monte Carlo simulations. We consider the scenario, where a team of $M = 4$ robots randomly move on a surface and track multiple targets with $N = 2$. While any type of motion and process model is applicable for the proposed algorithm, we adopt the unicycle model for both robots and targets, to be consistent with the ensuing experimental case. The robot pose $\mathbf{x}_{R_i}^k$ is described with the position $[x_{R_i}^k, y_{R_i}^k]$ and the orientation $\phi_{R_i}^k$ in the global frame. Then, the motion model is expressed as

$$\begin{aligned} x_{R_i}^k &= x_{R_i}^{k-1} + v_{R_i}^{k-1}\delta t\cos(\phi_{R_i}^{k-1}) \\ y_{R_i}^k &= y_{R_i}^{k-1} + v_{R_i}^{k-1}\delta t\sin(\phi_{R_i}^{k-1}) \\ \phi_{R_i}^k &= \phi_{R_i}^{k-1} + \omega_{R_i}^{k-1}\delta t \end{aligned} \tag{30}$$

where δt is the length of the sampling time interval, and v_{R_i}, ω_{R_i} represent, respectively, the linear and rotational velocity of robot i. These velocities are measured by the odometries equipped on the drive wheels and the associated noise is assumed to be white Gaussian with the standard deviation of 0.02 m for position and 2° for orientation. Each robot moves with a constant linear velocity of $v_{R_i} = 0.5$ m/s, and the rotational velocity ω_{R_i} is chosen from a uniform distribution over $[-(\pi/6), (\pi/6)]$ rad/s. Similarly, the targets move in the same area following the process of (30) with $v_{T_i} = 0.6$ m/s and $\omega_{T_i} \in [-(\pi/5), (\pi/5)]$ rad/s, subject to the same noise of the robot odometry measurements. The state $\mathbf{x}_{T_i}$ to be estimated contains the position and orientation of target i also in the global frame.

In the test, the robots and the targets start from different locations and follow the real trajectories depicted in Fig. 1. Although our approach can deal with generic measurement models, to be consistent with the experiment, each robot records the relative distance and bearing to other robots and targets within its sensing region. In order to fully validate our algorithm, in the simulation case no absolute measurements exist and the relative measurements are generated randomly in time, while in the following experimental case, the landmarks provide absolute measurements and the relative measurements
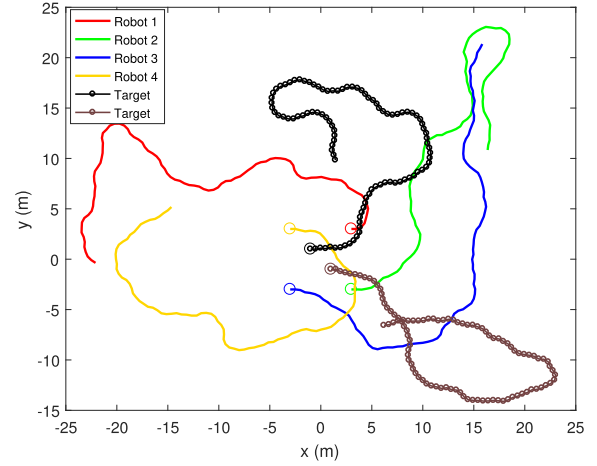

Fig. 1. Team of four robots move randomly and track two targets. Their starting positions are marked by circles.

obtained are related to the pose of each robot. For robot i, if robot j is detected, the relative measurement is given by

$$\mathbf{z}_{R_{ij}}^k = \begin{bmatrix} \sqrt{(x_{R_j}^k - x_{R_i}^k)^2 + (y_{R_j}^k - y_{R_i}^k)^2} \\ \text{atan2}((y_{R_j}^k - y_{R_i}^k), (x_{R_j}^k - x_{R_i}^k)) - \phi_{R_i}^k \end{bmatrix} + \mathbf{v}_{R_{ij}}^k$$

where $\mathbf{v}_{R_{ij}}$ is a zero-mean white Gaussian noise. The distance noise is set to be 3% of the actual value and the standard deviation of the bearing noise equals to 3°. The same model is used for the robot-to-target measurement $\mathbf{z}_{T_{ij}}$.

Consider a general case in which each robot performs relative measurements to the other robots with a probability of 20%, while the probability of detecting the targets is 40%. We consider a weak communication link with a failure probability of 30% between each pair. Since the absolute measurement is not accessible, we assume that each robot knows its initial global pose. The initial estimates of the targets' states obtained by each robot are set to $\hat{\mathbf{x}}_{T_{ij}}^0 \sim \mathcal{N}(\mathbf{x}_{T_j}(0), \mathbf{p}_{T_{ij}}^0)$, where $\mathbf{x}_{T_j}(0)$ is the initial true state of the target, and the initial covariance $\mathbf{p}_{T_{ij}}^0 = \mathbf{I}_3$, for $j = 1, 2$. We run 50 Monte Carlo simulations and compare the following four cases under the same setup.

1) Dead reckoning (DR): No relative measurements exist. The robots propagate their estimates by integrating the measured velocities. Target tracking is not considered here, since good knowledge of the robots' poses is a prerequisite for tracking.

2) CL-DEIF: To show the strength of jointly estimating the states of robots and targets, we purposely neglect the existence of targets and perform CL using the novel DEIF in Table I without incorporating robot-to-target measurements.

3) JLATT-DEIF: Based on the algorithms of Tables I and II, we achieve localization and target tracking simultaneously.

4) CEKF: To the best of our knowledge, none of the existing works can address the same problem in a fully distributed way. We, hence, use CEKF as the benchmark. The centralized state vector contains all the robots' and
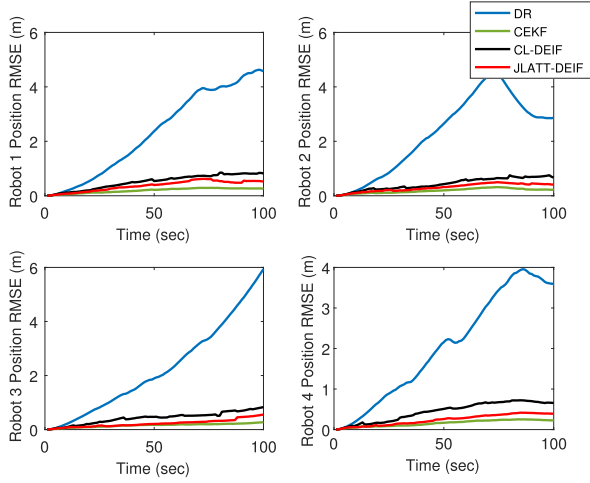
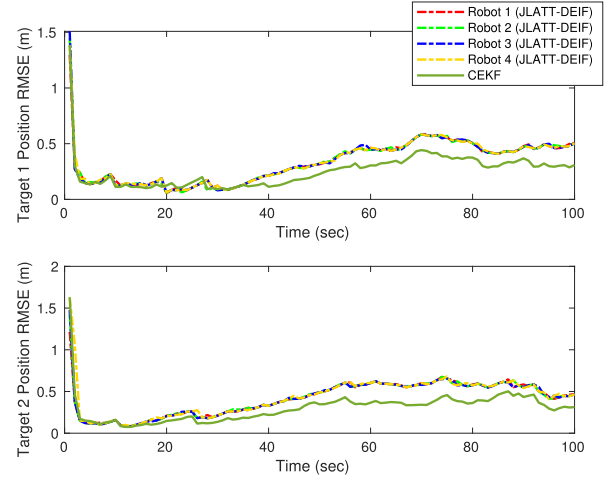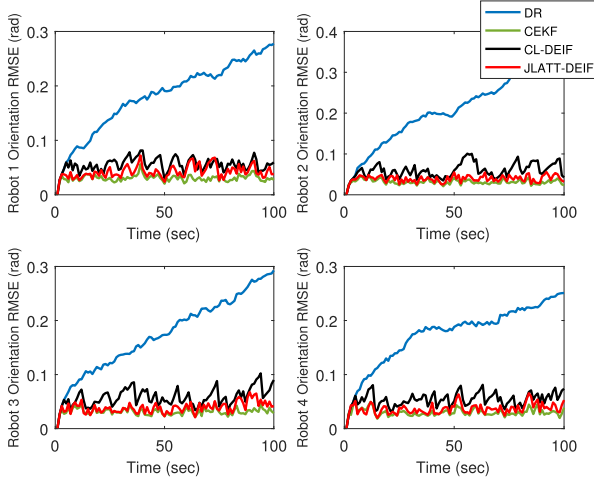Fig. 2. Position RMSE for four robots averaged over 50 Monte Carlo runs.

Fig. 3. Orientation RMSE for four robots averaged over 50 Monte Carlo runs.

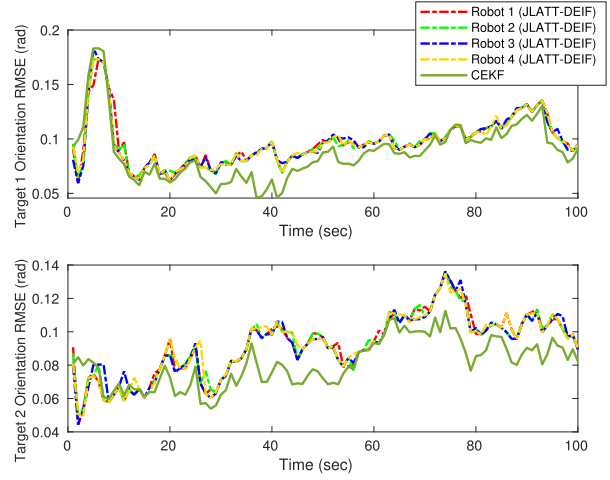Fig. 4. Position RMSE for two targets averaged over 50 Monte Carlo runs.

Fig. 5. Orientation RMSE for two targets averaged over 50 Monte Carlo runs.

targets' states. Whenever a relative measurement occurs, the EKF-based update invokes.

We employ the root-mean-square error (RMSE) to quantify the accuracy. Figs. 2 and 3 show the average RMSE over 50 Monte Carlo runs in positions and orientations for the four robots. As expected, without relative measurements, the estimation errors of DR increase quickly as time goes on. When relative measurements take place in the other three cases, due to the collected information regarding the relative motion to the other robots and targets, the pose uncertainties are significantly reduced. It is evident that JLATT-DEIF results in better accuracy for the estimates of both robot positions and orientations, compared with CL-DEIF in which robot-to-target measurements are ignored. Figs. 4 and 5 show the position and orientation RMSE for the state estimates of two targets obtained by four robots using JLATT-DEIF and the benchmark CEKF. It becomes clear that four robots can track the targets with performance close to CEKF through communicating only with one-hop neighbors. In comparison with CEKF, which achieves the best accuracy, the errors of JLATT-DEIF are slightly larger in both localization and

tracking. This is due to the fact that each robot only uses the information from itself and one-hop communicating neighbors. However, it allows for a fully distributed implementation with less computational and communication costs while preserving consistency.

To illustrate the consistency issue considered in Section III, we show how the algorithm would perform if the update steps in Tables I and II are replaced with, respectively, (18) and (23). The resulting algorithm is denoted as the *inconsistent JLATT-DEIF* (iJLATT-DEIF) and is then compared with the JLATT-DEIF. The normalized estimation error squared (NEES) [32] is used to evaluate the filter consistency. Specifically, if a filer is consistent, it is expected that the average NEES overall Monte Carlo runs for both robots' and targets' states will be close to 3 (i.e., should be close to the dimension of the state errors). A larger NEES value indicates inconsistency. Fig. 6 shows the average NEES for the estimates of one robot and one target. We note that the average NEES of the JLATT-DEIF is close to that of the benchmark CEKF and the ideal value 3 in both the localization and tracking parts. While the average NEES of the iJLATT-DEIF in these two parts is
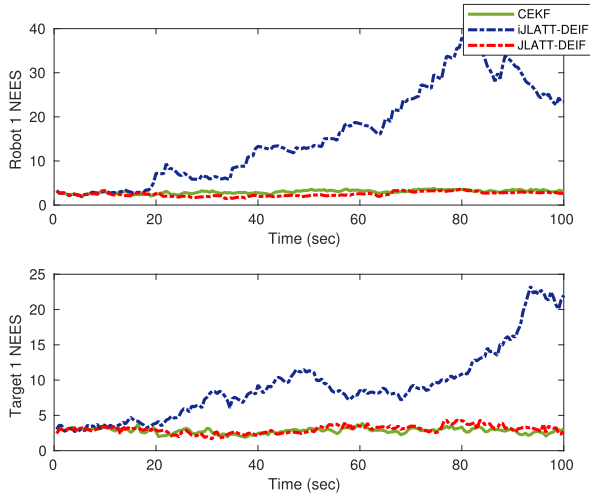
Fig. 6.   Average NEES for Robot 1 and Target 1 (obtained by Robot 1) averaged over 50 Monte Carlo runs.

gradually increasing over time, indicating that the estimates become inconsistent quickly.

VI. EXPERIMENT WITH REAL-WORLD DATA

We further evaluate the performance of our approach on the publically available *UTIAS multirobot CL and mapping data set* [33], where a fleet of five ground robots move in an indoor area of 15 m × 8 m with 15 static landmarks. Each robot is equipped with a monocular camera with a field of view (FOV) of about 60°. The robot makes range and bearing measurements when another robot or landmark is inside its FOV. In the meanwhile, a Vicon system is used to monitor the robots' poses and the positions of the landmarks, serving as the ground truth in the global frame. Note that the original intention of the data set is not for target tracking. In order to test our approach, we treat one of the robots as the target whose exteroceptive measurements are dropped and the other four forms a robot network. We sample the logged data at 50 Hz. In the data set, there are numerous occlusions between the robots and the target assigned for our purpose, which does not allow the recovering of the target trajectory. To test the target tracking scenario, the ground truth is used to synthesize robot-to-target measurements with the accuracy of 1% of the actual value for the position and 1° for bearing. Note that the synthesized data is only incorporated in the tracking part. Table III gives an overview on the number of actual measurements (including odometry data and relative and absolute measurements obtained by cameras), and the synthesized robot-to-target measurements for each robot within the first 30 000 time instants. The values in parentheses are the actual robot-to-target measurements.

The initial estimates for the robot poses are obtained by adding (or subtracting) 0.5-m offset to (or from) the true positions and 5° to (or from) the true orientation, rather than the true poses in the preceding simulation. For each robot, the target state estimate is initialized at $\hat{\mathbf{x}}_{R_i,1}^0 \sim \mathcal{N}(\mathbf{x}_{T_1}(0), \mathbf{p}_{R_i,1}^0)$, where $\mathbf{p}_{R_i,1}^0 = 0.5\mathbf{I}_3$. As in the preceding simulation test, we compare the performance of our approach

TABLE III
OVERVIEW OF HOW MANY MEASUREMENTS ARE USED

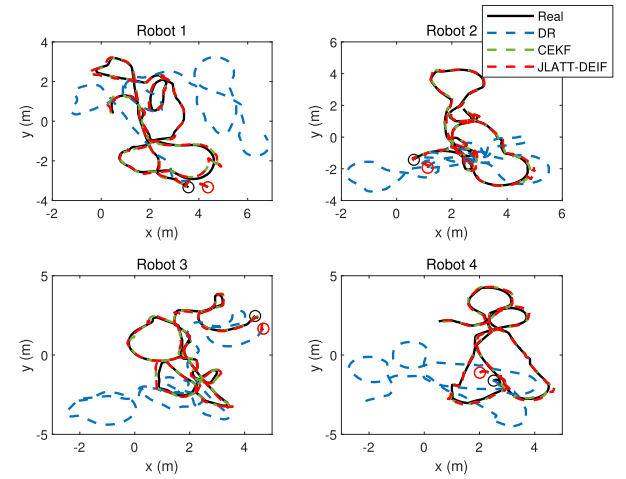|	Actual Measurement		Synthesized Measurement
_	Odometry	Camera	(robot-to-target)
Robot 1	30000	2184 (124)	297
Robot 2	30000	2424 (136)	272
Robot 3	30000	2874 (153)	259
Robot 4	30000	3530 (155)	267

Fig. 7.   Trajectories of four robots. In these lines, the black solid lines correspond to the real value, the blue dashed lines to DR, the green dashed lines to CEKF, and the red dashed lines to JLATT-DEIF. The initial true and estimated positions are marked by circles with the corresponding colors. Circles of DR, CEKF, and JLATT-DEIF are overlapped for each robot.
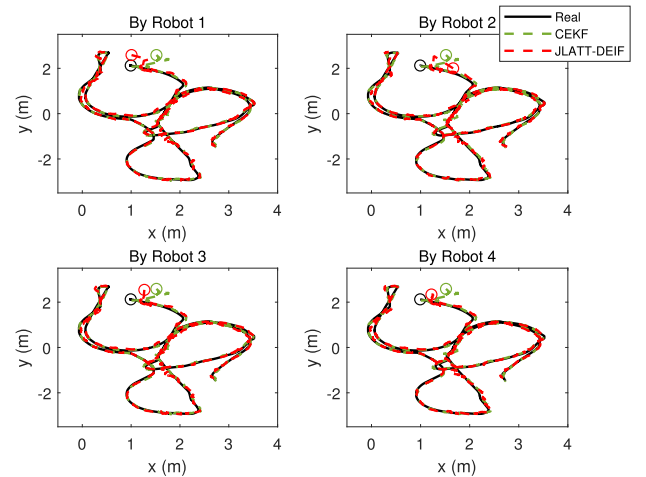

Fig. 8.   Trajectories of the target obtained by four robots. In these lines, the black solid lines correspond to the real value, the green dashed lines to CEKF, and the red dashed lines to JLATT-DEIF. The initial true and estimated positions are marked by circles with the corresponding colors.

JLATT-DEIF with the benchmark CEKF and the DR. Fig. 7 shows the real and estimated trajectories for the robots and Fig. 8 shows the results of the target estimates obtained by four robots over the first 30 000-time instants. It becomes clear that each robot's estimate of its own position (respectively,
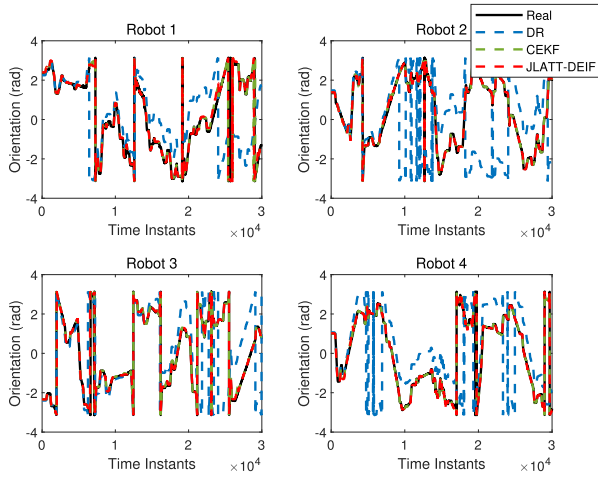
Fig. 9. Orientations for four robots. In these lines, the black solid lines correspond to the real value, the blue dashed lines to DR, the green dashed lines to CEKF, and the red dashed lines to JLATT-DEIF.
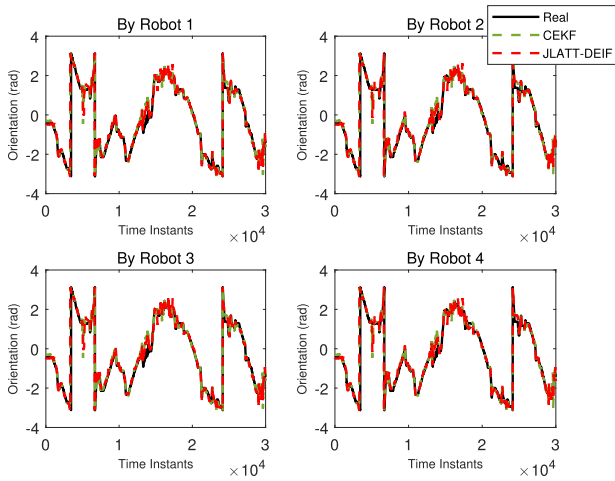

Fig. 10. Orientations for the target obtained by four robots. In these lines, the black solid lines correspond to the real value, the green dashed lines to CEKF, and the red dashed lines to JLATT-DEIF.
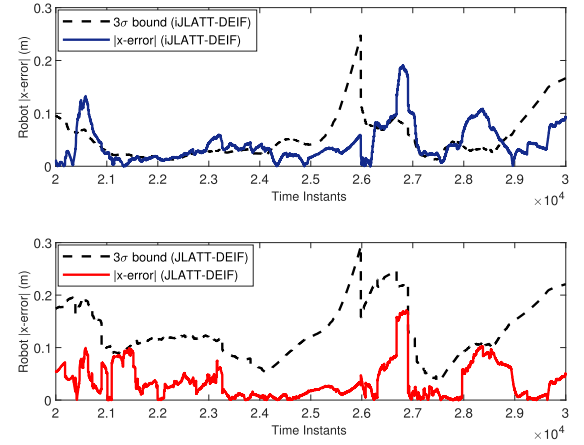

Fig. 11. Position error in the x-direction for one of the robots by using iJLATT-DEIF (top) and JLATT-DEIF (bottom). The solid lines correspond to the absolute value of x errors and the dashed lines to the 3σ bounds.
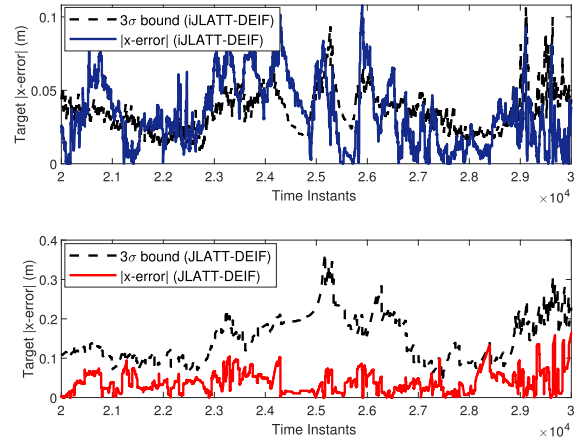

Fig. 12. Position error in the x-direction for the target by using iJLATT-DEIF (top) and JLATT-DEIF (bottom). The solid lines correspond to the absolute value of x errors and the dashed lines to the 3σ bounds.

the target's position) well tracks the real trajectory of its own (respectively, the target) without knowing the initial true pose. Furthermore, as shown in Figs. 9 and 10, each robot can also well estimate the real orientations of itself and the target. This is due to the existence of the landmarks, which provide the robots with intermittent absolute information in addition to the relative measurements. Furthermore, the proposed JLATT-DEIF performs comparably to CEKF and the ground truth.

Fig. 11 presents the recorded absolute value of x errors for one of the robots and the 3σ bound for these errors over a time interval of 10 000 instants. The top plot shows the result for iJLATT-DEIF. There are some time intervals in which the absolute x error is outside the 3σ bound, a clear indication that the iJLATT-DEIF estimate is overconfident, which may cause the estimate to diverge. Unlike that, in the bottom one, the resulting absolute x error of JLATT-DEIF is well enveloped by the 3σ bound, which agrees with the

previous simulation result that JLATT-DEIF is consistent in the localization part. Fig. 12 shows the comparative result along the x-direction for one target. Note that robot-to-target measurements have been incorporated in the localization part. Hence, directly using (23) leads to an inconsistent estimate, as shown in the top plot. While as shown in the bottom one, JLATT-DEIF also computes consistent estimates in the tracking part.

VII. CONCLUSION

In this article, we have introduced a fully distributed algorithm for the problem of JLATT when both the sensor network and the targets are mobile. Each robot maintains only the latest estimates of its own pose and the states of the targets. The proposed algorithm only requires one communication iteration with the nearby neighbors at one time instant. Furthermore, our approach supports generic robot motion, target process and measurement models, changing communication topologies, and dynamic blind robots. These properties ensure that our approach is applicable in a wide range of multirobot scenarios. We have also theoretically justified that the proposed estimates

are consistent and stable, with the errors being bounded in the linearized case. The effectiveness of our approach has been validated by using Monte Carlo simulations and the real-world data set in different scenarios.

REFERENCES

[1] S. I. Roumeliotis and G. A. Bekey, "Distributed multirobot localization," *IEEE Trans. Robot. Autom.*, vol. 18, no. 5, pp. 781–795, Oct. 2002.

[2] S. S. Kia, S. F. Rounds, and S. Martinez, "A centralized-equivalent decentralized implementation of extended Kalman filters for cooperative localization," in *Proc. IEEE/RSJ Int. Conf. Intell. Robots Syst.*, Sep. 2014, pp. 3761–3766.

[3] T. Bailey, M. Bryson, H. Mu, J. Vial, L. McCalman, and H. Durrant-Whyte, "Decentralised cooperative localisation for heterogeneous teams of mobile robots," in *Proc. IEEE Int. Conf. Robot. Autom.*, May 2011, pp. 2859–2865.

[4] T. R. Wanasinghe, G. K. I. Mann, and R. G. Gosine, "Distributed leader-assistive localization method for a heterogeneous multirobotic system," *IEEE Trans. Autom. Sci. Eng.*, vol. 12, no. 3, pp. 795–809, Jul. 2015.

[5] A. Martinelli, "Improving the precision on multi robot localization by using a series of filters hierarchically distributed," in *Proc. IEEE/RSJ Int. Conf. Intell. Robots Syst.*, Oct. 2007, pp. 1053–1058.

[6] S. Panzieri, F. Pascucci, and R. Setola, "Multirobot localisation using interlaced extended Kalman filter," in *Proc. IEEE/RSJ Int. Conf. Intell. Robots Syst.*, Oct. 2006, pp. 2816–2821.

[7] L. Luft, T. Schubert, S. I. Roumeliotis, and W. Burgard, "Recursive decentralized localization for multi-robot systems with asynchronous pairwise communication," *Int. J. Robot. Res.*, vol. 37, no. 10, pp. 1152–1167, Sep. 2018.

[8] L. C. Carrillo-Arce, E. D. Nerurkar, J. L. Gordillo, and S. I. Roumeliotis, "Decentralized multi-robot cooperative localization using covariance intersection," in *Proc. IEEE/RSJ Int. Conf. Intell. Robots Syst.*, Nov. 2013, pp. 1412–1417.

[9] A. Bahr, M. R. Walter, and J. J. Leonard, "Consistent cooperative localization," in *Proc. IEEE Int. Conf. Robot. Autom.*, May 2009, pp. 3415–3422.

[10] R. Olfati-Saber, "Distributed Kalman filtering for sensor networks," in *Proc. 46th IEEE Conf. Decis. Control*, Oct. 2007, pp. 5492–5498.

[11] A. T. Kamal, J. A. Farrell, and A. K. Roy-Chowdhury, "Information weighted consensus filters and their application in distributed camera networks," *IEEE Trans. Autom. Control*, vol. 58, no. 12, pp. 3112–3125, Dec. 2013.

[12] W. Ren, R. W. Beard, and D. B. Kingston, "Multi-agent Kalman consensus with relative uncertainty," in *Proc. Amer. Control Conf.*, 2005, pp. 1865–1870.

[13] G. Battistelli and L. Chisci, "Kullback–Leibler average, consensus on probability densities, and distributed state estimation with guaranteed stability," *Automatica*, vol. 50, no. 3, pp. 707–718, Mar. 2014.

[14] R. Olfati-Saber, "Kalman-consensus filter: Optimality, stability, and performance," in *Proc. 48th IEEE Conf. Decision Control (CDC)*, Dec. 2009, pp. 7036–7042.

[15] G. Battistelli, L. Chisci, G. Mugnai, A. Farina, and A. Graziano, "Consensus-based linear and nonlinear filtering," *IEEE Trans. Autom. Control*, vol. 60, no. 5, pp. 1410–1415, May 2015.

[16] S. Wang and W. Ren, "On the convergence conditions of distributed dynamic state estimation using sensor networks: A unified framework," *IEEE Trans. Control Syst. Technol.*, vol. 26, no. 4, pp. 1300–1316, Jul. 2018.

[17] F. S. Cattivelli and A. H. Sayed, "Diffusion strategies for distributed Kalman filtering and smoothing," *IEEE Trans. Autom. Control*, vol. 55, no. 9, pp. 2069–2084, Sep. 2010.

[18] J. Hu, L. Xie, and C. Zhang, "Diffusion Kalman filtering based on covariance intersection," *IFAC Proc. Volumes*, vol. 44, no. 1, pp. 12471–12476, Jan. 2011.

[19] G. Huang, M. Kaess, and J. J. Leonard, "Consistent unscented incremental smoothing for multi-robot cooperative target tracking," *Robot. Auto. Syst.*, vol. 69, pp. 52–67, Jul. 2015.

[20] A. Ahmad, G. D. Tipaldi, P. Lima, and W. Burgard, "Cooperative robot localization and target tracking based on least squares minimization," in *Proc. IEEE Int. Conf. Robot. Autom.*, May 2013, pp. 5696–5701.

[21] F. M. Mirzaei, A. I. Mourikis, and S. I. Roumeliotis, "On the performance of multi-robot target tracking," in *Proc. IEEE Int. Conf. Robot. Autom.*, Apr. 2007, pp. 3482–3489.

[22] N. Atanasov, R. Tron, V. M. Preciado, and G. J. Pappas, "Joint estimation and localization in sensor networks," in *Proc. 53rd IEEE Conf. Decis. Control*, Dec. 2014, pp. 6875–6882.

[23] P. Zhu and W. Ren, "Multi-robot joint localization and target tracking with local sensing and communication," in *Proc. Amer. Control Conf. (ACC)*, Jul. 2019, pp. 3261–3266.

[24] S. J. Julier and J. K. Uhlmann, "A non-divergent estimation algorithm in the presence of unknown correlations," in *Proc. Amer. Control Conf.*, 1997, pp. 2369–2373.

[25] P. S. Maybeck, *Stochastic Models, Estimation, and Control*, vol. 3. New York, NY, USA: Academic, 1982.

[26] P. O. Arambel, C. Rago, and R. K. Mehra, "Covariance intersection algorithm for distributed spacecraft state estimation," in *Proc. Amer. Control Conf.*, 2001, pp. 4398–4403.

[27] Y. Bar-Shalom and L. Campo, "The effect of the common process noise on the two-sensor fused-track covariance," *IEEE Trans. Aerosp. Electron. Syst.*, vols. AES–22, no. 6, pp. 803–805, Nov. 1986.

[28] B. Noack, J. Sijs, M. Reinhardt, and U. D. Hanebeck, "Decentralized data fusion with inverse covariance intersection," *Automatica*, vol. 79, pp. 35–41, May 2017.

[29] S. Julier and J. K. Uhlmann, "General decentralized data fusion with covariance intersection," in *Handbook Multi Sensor Data Fusion*. Boca Raton, FL, USA: CRC Press, 2017, pp. 339–364.

[30] W. Niehsen, "Information fusion based on fast covariance intersection filtering," in *Proc. 5th Int. Conf. Inf. Fusion. Fusion*, Oct. 2002, pp. 901–904.

[31] S. Wang, Y. Lyu, and W. Ren, "Unscented-transformation-based distributed nonlinear state estimation: Algorithm, analysis, and experiments," *IEEE Trans. Control Syst. Technol.*, vol. 27, no. 5, pp. 2016–2029, Sep. 2019.

[32] Y. Bar-Shalom, X. R. Li, and T. Kirubarajan, *Estimation With Applications to Tracking and Navigation: Theory Algorithms and Software*. Hoboken, NJ, USA: Wiley, 2004.

[33] K. Y. Leung, Y. Halpern, T. D. Barfoot, and H. H. Liu, "The UTIAS multi-robot cooperative localization and mapping dataset," *Int. J. Robot. Res.*, vol. 30, no. 8, pp. 969–974, Jul. 2011.

Pengxiang Zhu received the B.Eng. and M.S. degrees in control science and engineering from Harbin Engineering University, Harbin, China, in 2013 and 2016, respectively. He is currently pursuing the Ph.D. degree in electrical engineering with the University of California at Riverside, Riverside, CA, USA. His current research interests include state estimation, sensor fusion, and visual-inertial navigation for autonomous robots.
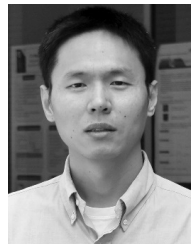
Wei Ren (Fellow, IEEE) received the Ph.D. degree in electrical engineering from Brigham Young University, Provo, UT, USA, in 2004.

He was a Faculty Member with Utah State University, Logan, UT, USA, and a Post-Doctoral Research Associate with the University of Maryland, College Park, MD, USA. He is currently a Professor with the Department of Electrical and Computer Engineering, University of California at Riverside, Riverside, CA, USA. His research focuses on distributed control of multi-agent systems and autonomous control of unmanned vehicles.

Dr. Ren was a recipient of the National Science Foundation CAREER Award in 2008 and the IEEE Control Systems Society Antonio Ruberti Young Researcher Prize in 2017. He is currently an IEEE Control Systems Society Distinguished Lecturer. He is an Associate Editor of the IEEE TRANSACTIONS ON AUTOMATIC CONTROL.